

of d^7-d^7 M_2X_2 complexes.¹⁴⁻¹⁶) Other chemical properties of Pt_2H_2 also are consistent with its formulation as a terminal dihydride. It reacts with HCl and DCl to generate H_2 and HD, respectively. Dioxygen reacts with Pt_2H_2 very rapidly with quantitative regeneration of Pt_2 . The spectroscopic evidence and the reaction with H^+ point to the formal oxidation state assignment $Pt_2^{III}(H^-)_2$, but the O_2 chemistry indicates that the molecule also can be viewed as a $Pt_2^{II}(H^*)_2$ species with the redox centers being the hydrido ligands. The H^* groups can be released (and potentially transferred to substrates) either chemically or photochemically in a manner not unlike the alkyl-radical chemistry^{17,18} of certain Co(III) complexes.

(15) Stiegman, A. E.; Miskowski, V. M.; Gray, H. B. *J. Am. Chem. Soc.* **1986**, *108*, 2781-2782.

(16) Kurmoo, M.; Clark, R. J. H. *Inorg. Chem.* **1985**, *24*, 4420-4425.

(17) Halpern, J. *Pure Appl. Chem.* **1983**, *55*, 1059-1068.

(18) Halpern, J. *B₁₂*; Dolphin, D., Ed.; Wiley: New York, 1982; Vol. 1, pp 501-542.

Acknowledgment. We thank Paul Haake and James Yesinowski for helpful discussions, Max Roundhill for a preprint of ref. 5, and David Smith for assistance with the NMR and IR experiments. E. L. H. is a National Science Foundation Fellow. This research was supported by National Science Foundation Grants CHE84-19828 (H.B.G.) and CHE84-40137 (NMR Facility).

Registry No. Pt_2H_2 , 80011-25-2; $[Bu_4N]_4[Pt_2(P_2O_5H_2)_4]$, 89462-52-2; Bu_3SnH , 688-73-3; $PhCH(OH)CH_2CH_3$, 93-54-9; $PhCH(OH)CH_3$, 98-85-1; H_2 , 1333-74-0; HCl, 7647-01-0; O_2 , 7782-44-7.

Supplementary Material Available: Hand simulation of a satellite arising from the asymmetric isotopomer (spin system AA'XX'X''X'''X''''X'''''X''''''M), computer simulations (with parameters) of all three isotopomers on analogous spin systems containing fewer ^{31}P nuclei (four to seven spins), and the experimental and simulated ^{31}P -decoupled 1H spectra (11 pages). Ordering information is given on any current masthead page.

Aromatic Nitration with Ion Radical Pairs $[ArH^+, NO_2^-]$ as Reactive Intermediates. Time-Resolved Studies of Charge-Transfer Activation of Dialkoxybenzenes

S. Sankararaman, W. A. Haney, and J. K. Kochi*

Contribution from the Department of Chemistry, University of Houston, University Park, Houston, Texas 77004. Received February 3, 1987

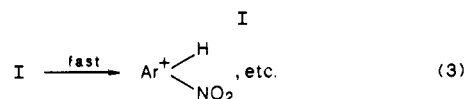
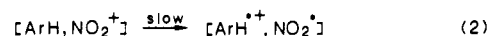
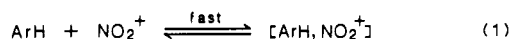
Abstract: Aromatic nitrations carried out both under electrophilic conditions and by charge-transfer activation afford the same yields and isomer distributions of nitration products from a common series of aromatic ethers (ArH). Time-resolved spectroscopy establishes the charge-transfer nitration to proceed via the ion radical pair $[ArH^+, NO_2^-]$, generated by the deliberate excitation of the electron donor-acceptor or π complex of the arene with $C(NO_2)_4$. Laser flash photolysis of the charge-transfer band defines the evolution of the arene cation radical ArH^+ and allows its decay kinetics to be delineated in various solvents and with added salts. The internal trapping of ArH^+ is examined in the substituted *p*-dimethoxybenzenes $CH_3OC_6H_4OCH_2X$ with $X = CO_2H, CO_2^-, CO_2Et,$ and CH_2OH as the pendant functional groups. The mechanistic relevance of the collapse of $[ArH^+, NO_2^-]$ to the Wheland intermediate is discussed in the context of electrophilic aromatic nitrations.

The idea that charge transfer may play a key role in aromatic nitration with nitronium ion was first suggested in 1945 by Kenner,¹ who envisaged an initial step that "involves transference of a π -electron...". Later Brown² postulated charge-transfer complexes as intermediates, and Nagakura³ provided further theoretical support for one-electron transfer between an aromatic donor (ArH) and an electrophile such as NO_2^+ . Despite notable elaborations by Pederson,⁴ Perrin,⁵ Ebersson,⁶ and others, this formulation has not been widely accepted for nitration and related electrophilic aromatic substitutions.⁷

As broadly conceived, the seminal question focusses on the activation process(es) leading up to the well-established Wheland

or σ -intermediate.^{8,9} In the electron-transfer mechanism, the formation of the ion radical I is the distinctive feature, as summarized in Scheme I.¹⁰ Accordingly, the properties and behavior

Scheme I



of the intimate ion radical pair I are crucial to establishing its relationship with the numerous facets^{11,12} of electrophilic aromatic

(1) Kenner, J. *Nature (London)* **1945**, *156*, 369.

(2) Brown, R. D. *J. Chem. Soc.* **1959**, 2224, 2232.

(3) (a) Nagakura, S.; Tanaka, J. *J. Chem. Phys.* **1954**, *22*, 563. (b) Nagakura, S. *Tetrahedron* **1963**, *19* (Suppl. 2), 361.

(4) Pederson, E. B.; Petersen, T. E.; Torsell, K.; Lawesson, S.-O. *Tetrahedron* **1973**, *29*, 579.

(5) Perrin, C. L. *J. Am. Chem. Soc.* **1977**, *99*, 5516.

(6) (a) Ebersson, L.; Jönsson, L.; Radner, F. *Acta Chem. Scand.* **1978**, *B32*, 749. (b) Ebersson, L.; Radner, F. *Acta Chem. Scand.* **1980**, *B34*, 739. (c) Ebersson, L.; Radner, F. *Acta Chem. Scand.* **1985**, *B39*, 357. (d) Ebersson, L.; Radner, F. *Acta Chem. Scand.* **1984**, *B38*, 861 and related papers.

(7) For an excellent review, see: Schofield, K. *Aromatic Nitration*; Cambridge University Press: Cambridge, 1980.

(8) Wheland, G. W. *J. Am. Chem. Soc.* **1942**, *64*, 900.

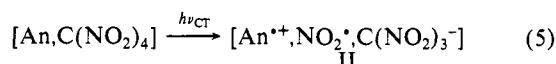
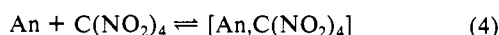
(9) See also: (a) Ingold, C. K. *Structure and Mechanism in Organic Chemistry*, 2nd ed.; Cornell University Press: Ithaca, NY, 1969. (b) Olah, G. A. In *Industrial and Laboratory Nitrations*; Albright, L. F., Hanson, C. Eds.; American Chemical Society: Washington, D.C. 1976; ACS Sym. Ser. 22. (c) Brower, D. M.; Mackor, G. L.; McLean, C. In *Carbonium Ions*; Olah, G., Schleyer, P. v. R., Eds.; Wiley: New York, 1970; Vol. 2.

(10) The brackets denote a loose (encounter) complex or solvent-caged species.

nitration. For these reasons it is especially important to know whether I will actually lead to the appropriate Wheland intermediates, and in the amounts necessary to establish the isomer distributions commonly observed in aromatic nitrations. However, the independent proof of the ion radical pair has not been forthcoming owing to its expectedly transitory character.¹³ Thus the arene ion radical pair cannot be observed in Scheme I, since its rate of annihilation will always be faster than its rate of production. An alternative approach is clearly required to test the viability of Scheme I.

We recently demonstrated that ion radical pairs are spontaneously generated from the photoactivation of electron donor-acceptor or EDA complexes.¹⁴ Relevant to the problem of aromatic nitration, the pertinent ion radical pair II was produced in essentially the ground state by the direct irradiation of the charge-transfer (CT) band of the π -complex of the arene anthracene (An) with tetranitromethane¹⁵ (see Scheme II).

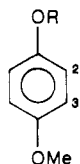
Scheme II



We wish to establish how an arene ion radical pair such as II can lead to aromatic substitution, hereafter referred to as charge-transfer nitration.¹⁶ The studies in this report are deliberately restricted to arenes derived from a series of dialkoxybenzenes, particularly those related to 1,4-dimethoxybenzene since (a) the stoichiometries in both electrophilic and charge-transfer nitrations are unambiguous, (b) the arene cation radicals ($\text{ArH}^{\cdot+}$) are known, (c) there are no *ipso* substitutions,¹⁷ and (d) subtle changes in the alkoxy group provide a sensitive probe for isomer distributions.

Results

I. Comparison of Electrophilic and Charge-Transfer Aromatic Nitration. Products and Stoichiometry. The series of related 1,4-dialkoxybenzenes were prepared by the reported procedures (see Experimental Section) and nitrated under both standard electrophilic and charge-transfer conditions. When $\text{R} \neq \text{CH}_3$,



R	
CH ₃	DMB
CH ₂ COOH	MPA
CH ₂ CO ₂ Et	EMP
CH ₂ CH ₂ OH	MPE

a pair of isomeric mononitro derivatives is possible. The structural assignments of the 2-nitro and 3-nitro isomers were readily based on the effect of the electronegative NO₂ group on the chemical shifts of the OCH₃ and OCH₂X groups in the ¹H NMR spectrum with X = CO₂H, CO₂Et, and CH₂OH. Thus the methylene protons in the 2-NO₂ isomers were consistently shifted downfield by ~0.1 ppm relative to those in the parent arenes.¹⁸ Similarly

Table I. Structural Assignment of the Isomeric Nitroaromatic Ethers from the ¹H NMR Spectra^a

R						
	δ_{CH_2}	δ_{CH_3}	δ_{CH_2}	δ_{CH_3}	δ_{CH_2}	δ_{CH_3}
CH ₃		3.77		3.81		3.91
CH ₂ COOH ^b	4.60	3.71	4.84	3.84	4.78	3.91
CH ₂ COOEt	4.55	3.75	4.70	3.82	4.62	3.92
CH ₂ CH ₂ OH	3.99 ^c	3.76	4.18	3.80	4.02	3.91
CH ₂ CD ₂ OH	4.01	3.76	4.16	3.81	4.05	3.90

^aIn CDCl₃ with Me₄Si internal reference. ^bIn acetone-*d*₆. ^cCenter of the multiplet.

Table II. Electrophilic Nitration of Aromatic Ethers with Nitric Acid.^a Products and Stoichiometry

ArH	isomer distribution (%) ^b				yield (%) ^c
	2-NO ₂	3-NO ₂	4-NO ₂	5-NO ₂	
	100				100
		0	100		82
	30	70			90
	30	70			95
	55	45			100
	55	45			100
	100		0	0	94
	100			0	80

^aIn glacial acetic acid at 0–25 °C. ^bBy ¹H NMR analysis. ^cBy isolation.

the methyl resonances in the 3-NO₂ isomers were always shifted ~0.1 ppm downfield due to the presence of the ortho nitro groups (see Table I).¹⁹ This basis for the structural assignments was confirmed by a systematic study of EMP with the shift reagent Eu(fod)₂, as described in the Experimental Section.

A. Electrophilic nitrations were carried out by treating the arene with 1 equiv of nitric acid in glacial acetic acid at 0–25 °C, as recommended by Clark.²⁰ Under these very mild conditions, the nitration occurred quantitatively according to the classical stoichiometry, i.e.



The isomer distributions of the 2- and 3-nitro derivatives obtained from all the 1,4-dialkoxybenzenes are listed in Table II together with the nitration products obtained from related aromatic ethers.

B. Charge-transfer nitrations were carried out simply by the actinic irradiation of aromatic solutions containing excess tetranitromethane (TNM) at 25 °C. The use of a Pyrex cutoff filter which rejected light with $\lambda < 425$ nm ensured that only the charge-transfer band (vide infra) of the EDA complex was excited. For example, after a solution of 0.4 M 1,4-dimethoxybenzene and

(19) See: Abraham, R. J.; Loftus, P. *Proton and Carbon-13 NMR Spectroscopy*; Heyden: London, 1978; p 28.

(20) Clark, E. P. *J. Am. Chem. Soc.* **1931**, *53*, 3431.

(11) Hartshorn, S. R. *Chem. Soc. Rev.* **1974**, *3*, 167.

(12) Suzuki, H. *Synthesis* **1977**, 217.

(13) For previous attempts to directly examine the reactions of various salts of $\text{ArH}^{\cdot+}$ and N_2O_4 , see Ebersohn⁶ and Perrin.⁵

(14) Hilinski, E. F.; Masnovi, J. M.; Kochi, J. K.; Rentzepis, P. M. *J. Am. Chem. Soc.* **1984**, *106*, 8071.

(15) Masnovi, J. M.; Kochi, J. K.; Hilinski, E. F.; Rentzepis, P. M. *J. Am. Chem. Soc.* **1986**, *108*, 1126.

(16) For a preliminary report, see: Sankararaman, S.; Kochi, J. K. *Recl. Trav. Chim. Pays-Bas* **1986**, *105*, 278.

(17) Compare Fischer, A.; Fyles, D. L.; Henderson, G. N.; Mahasay, S. R. *Can. J. Chem.* **1986**, *64*, 1764.

(18) Or relative to the methyl protons in the nitroarene.

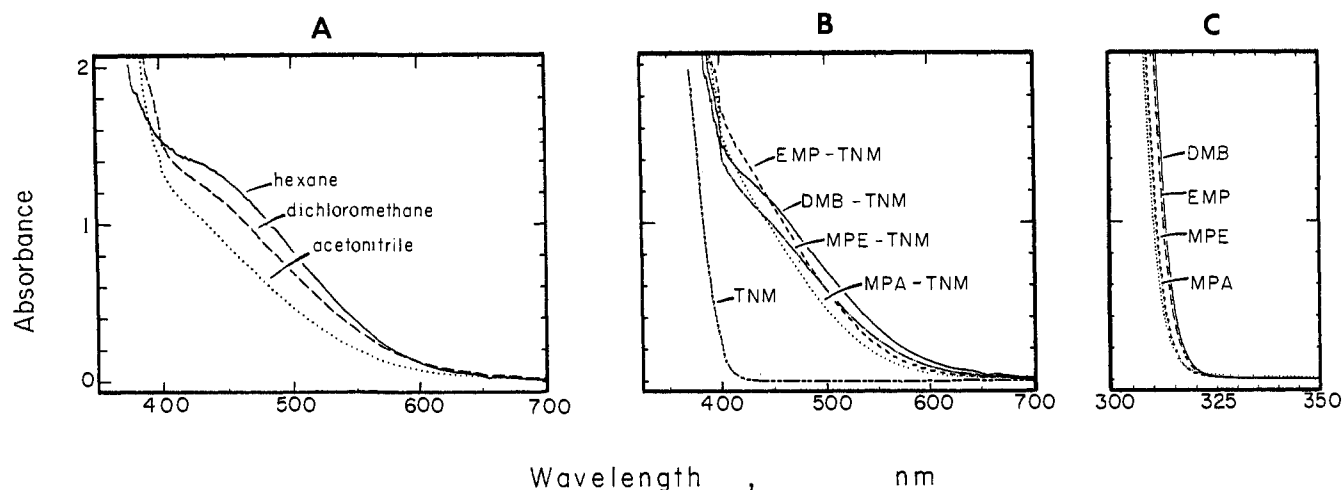
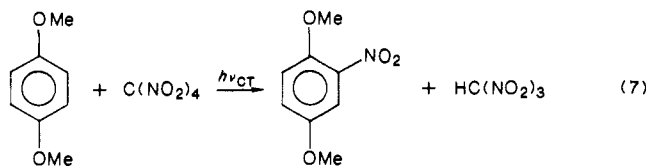
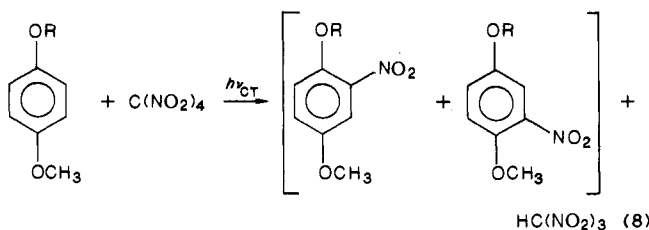


Figure 1. (A) Charge-transfer absorption spectra of the EDA complex of 0.05 M 1,4-dimethoxybenzene and ~0.5 M TNM in hexane (—), dichloromethane (---), and acetonitrile (···). (B) CT spectra of 0.05 M DMB (—), MPA (···), EMP (---), and MPE (---) with 1 M TNM in CH₂Cl₂. Absorption cutoff of TNM alone (·····). (C) Low-energy tails of 0.05 M DMB, MPA, EMP, and MPE in CH₂Cl₂.

1.5 M TNM in dichloromethane was irradiated, the analysis of the photolysate by gas chromatography indicated that all the DMB was consumed. A single aromatic product was isolated as 2,5-dimethoxynitrobenzene in 92% yield. Its spectral properties and GC-MS behavior coincided with those of an authentic sample.²¹ The trinitromethyl moiety was identified as nitroform by extraction of the crude reaction mixture dissolved in ether with water. The subsequent spectrophotometric analysis of the aqueous extract (see Experimental Section) indicated that 1 equiv of nitroform accompanied the formation of each mole of dimethoxynitrobenzene. Accordingly we deduce the complete stoichiometry of the CT photochemistry to be



The charge-transfer nitration of 2-(4-methoxyphenoxy)ethanol (MPE) and 4-methoxyphenoxyacetic acid (MPA) and its ethyl ester (EMP) carried out under similar conditions also resulted in essentially quantitative yields of a mixture of 2- and 3-nitro isomers, i.e.



The isomer distributions of the nitrated products are included in Table III for all the 1,4-dialkoxybenzenes, together with those of related aromatic ethers. No dinitration occurred under these reaction conditions.

In order to identify the photochemical process which led to charge-transfer nitration, we examined the spectral changes accompanying the exposure of the aromatic ethers to tetranitromethane.

II. Charge-Transfer Spectra of the EDA Complexes of Aromatic Ethers with Tetranitromethane as Reaction Intermediates. When tetranitromethane and 1,4-dimethoxybenzene were mixed, an instantaneous coloration was observed which varied from wine red to deep yellow depending on the concentrations of each component and the solvent. The corresponding changes in the

Table III. Charge-Transfer Nitration of Aromatic Ethers with Tetranitromethane.^a Products and Stoichiometry

ArH	solvent	isomer distribution (%) ^b				yield (%) ^c
		2-NO ₂	3-NO ₂	4-NO ₂	5-NO ₂	
	CH ₂ Cl ₂	100				93
	CH ₃ CN	100				100
	CH ₂ Cl ₂		0	100		98
	CH ₂ Cl ₂	30	70			98 ^d
	CH ₃ CN	30	70			100 ^d
	CH ₂ Cl ₂	30	70			93
	CH ₃ CN	30	70			100 ^d
	CH ₂ Cl ₂	75	25			85
	CH ₃ CN	60	40			96 ^d
	CH ₂ Cl ₂	75	25			96 ^d
	CH ₃ CN	60	40			96 ^d
	CH ₂ Cl ₂	100		0		93 ^d
	CH ₂ Cl ₂	100			0	94 ^d

^aBy irradiation at $\lambda > 425$ nm. ^bBy ¹H NMR analysis. ^cBy isolation, unless stated otherwise. ^dBy NMR analysis with internal standard (see Experimental Section).

absorption spectra are illustrated in Figure 1A. The colors attendant upon the exposure of the various aromatic ethers to TNM are clearly associated with appearance of these new absorption bands (Figure 1B), since neither tetranitromethane nor the aromatic ethers absorb in the visible region.

These broad absorption bands are characteristic of charge-transfer transitions associated with intermolecular electron donor-acceptor complexes.^{22,23} Such an assignment accords with the spectral blue shift that accompanied the increase in solvent polarity (Figure 1A) and the red shift relative to that observed with less-electron-rich arenes such as benzene, toluene, or anisole.^{24,25} Both trends are necessarily qualitative since the ab-

(22) Foster, R. *Organic Charge Transfer Complexes*; Academic: New York, 1969.

(23) Mulliken, R. S.; Person, W. B. *Molecular Complexes: A Lecture and Reprint Volume*; Wiley: New York, 1969.

(24) Altukhov, K. V.; Perekalin, V. V. *Russ. Chem. Rev.* **1976**, *45*, 1052.

(21) Ungnade, H. E.; Zilch, K. T. *J. Org. Chem.* **1951**, *16*, 68.

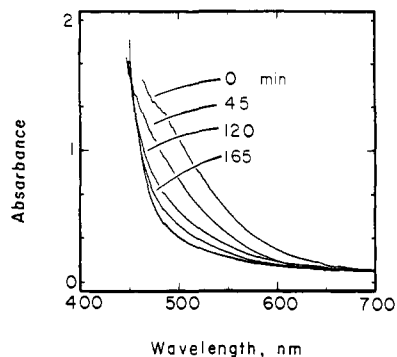


Figure 2. Typical bleaching of the CT band upon constant visible irradiation at $\lambda > 425$ nm, as shown for 0.2 M MPE and 0.3 M TNM after (top-to-bottom) 0, 45, 120, 165, 275, and 350 min.

sorption maxima of the CT bands are obscured by the low-energy tails of the uncomplexed aromatic ethers (Figure 1C) and TNM (Figure 1B). All of these CT bands persisted indefinitely at room temperature if the solutions were protected from adventitious exposure to room light. However, when these solutions were deliberately irradiated with visible light (filtered for $\lambda > 425$ nm), the monotonic decrease in the CT absorption bands (see Figure 2) was visually observed as the bleaching of the red-orange solution. The final yellow color was due to trinitromethide ($\lambda_{\max} = 350$ nm, $\epsilon_{\max} = 14000^{26}$) resulting from the acid dissociation of nitroform²⁷ (see eq 7 and 8). Thus the EDA complexes $[\text{Ar} \cdot \text{H}, \text{C}(\text{NO}_2)_4]$ are the precursors responsible for charge-transfer nitrations. As such, we inquire as to the amounts of the EDA complex that are present in solution.

Formation Constants of the EDA Complexes from Aromatic Ethers and TNM. The formation constant K of the EDA complexes of the various dialkoxybenzenes and tetranitromethane in dichloromethane was measured spectrophotometrically by the



Benesi-Hildebrand procedure.^{28,29} For the 1:1 complex in eq 9, the changes in the absorbance A_{CT} of the charge-transfer band at various concentrations of the aromatic donor and TNM are given by

$$\frac{[\text{ArH}]}{A_{\text{CT}}} = \frac{1}{\epsilon_{\text{CT}}} + \frac{1}{K\epsilon_{\text{CT}}[\text{TNM}]} \quad (10)$$

under conditions in which $[\text{TNM}] \gg [\text{ArH}]$. To avoid complications arising from higher order complexes,³⁰ all the spectral measurements were made with tetranitromethane in excess. Since only the absorption tails of the CT bands are observed in Figure 1, the absorbance was measured at two wavelengths, 450 and 460 nm. Each of the Benesi-Hildebrand plots consisted of 8 data points, and the resulting linear fit to eq 10 was consistently obtained by the method of least squares with a correlation coefficient > 0.995 (Figure 3). Some typical results collected at 450 and 460 nm are listed in Table IV. Within experimental error, the same values of K were obtained from spectral measurements made at 470 nm. The limited magnitudes of K in Table IV indicate that the EDA complexes of aromatic compounds with TNM are best classified as weak.³¹

(25) (a) Ostromyslensky, I. *J. Prakt. Chem.* **1911**, *84*, 1495. (b) Hammick, D. L.; Yule, R. B. *M. J. Chem. Soc.* **1940**, 1539. (c) Davies, T. T.; Hammick, D. L. *J. Chem. Soc.* **1938**, 763. (d) Rao, C. N. R. In *Chemistry of Nitro and Nitroso Groups*; Feuer, H., Ed.; Wiley: New York, 1969; Part 1, Chapter 2.

(26) Masnovi, J. M.; Kochi, J. K. *J. Am. Chem. Soc.* **1985**, *107*, 7880.

(27) For nitroform $\text{p}K_{\text{a}} \ll \text{som 0}$. Cram, D. J. *Fundamentals of Carbanion Chemistry*; Academic: New York, 1965.

(28) Benesi, H. A.; Hildebrand, J. H. *J. Am. Chem. Soc.* **1949**, *71*, 2703.

(29) (a) Person, W. B. *J. Am. Chem. Soc.* **1965**, *87*, 167. (b) Foster, R. *Molecular Complexes*; Crane, Russak & Co.: New York, 1974; Vol. 2.

(30) Masnovi, J. M.; Hilinski, E. F.; Rentzepis, P. M.; Kochi, J. K. *J. Phys. Chem.* **1985**, *89*, 5387.

(31) Mulliken, R. S. *J. Am. Chem. Soc.* **1952**, *74*, 811. See also Foster.²²

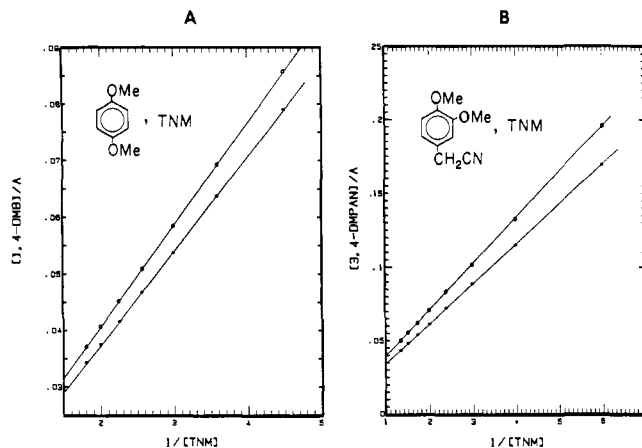
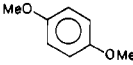
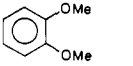
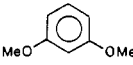
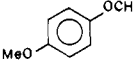
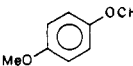
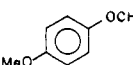
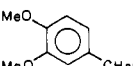
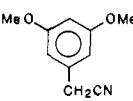


Figure 3. Spectrophotometric determination of the formation constant K of the EDA complexes by the Benesi-Hildebrand method, as typical shown for (A) 0.05 M DMB and (B) 0.05 M 3,4-dimethoxyphenylacetonitrile with 0.16–0.55 M TNM in CH_2Cl_2 at the monitoring wavelengths 450 (*) and 460 (O) nm.

Table IV. Formation Constants of the EDA Complexes of Aromatic Ethers and Tetranitromethane^a

ArH	ϵ ($\text{M}^{-1} \text{cm}^{-1}$)	K (M^{-1})
	234 (270)	0.23 (0.22)
	164 (190)	0.26 (0.25)
	46 (48)	0.29 (0.28)
	135 (157)	0.25 (0.25)
	144 (167)	0.27 (0.26)
	166 (179)	0.28 (0.28)
	115 (127)	0.27 (0.28)
	101 (136)	0.31 (0.25)

^a In dichloromethane at 25 °C and measured at 450 nm and (460 nm).

Time-Resolved Absorption Spectra of the Transient Intermediates in Charge-Transfer Nitration. The photobleaching of the CT absorption band in Figure 2 was examined more closely by time-resolved spectroscopy. The laser excitation was carried out at 532 nm with a 25-ps pulse derived from the frequency-doubled output of a mode-locked Nd^{3+} :YAG oscillator.³² This excitation pulse corresponded to only the tails of the CT absorption bands (see Figure 1). Thus there is no ambiguity about either the adventitious local excitation of the uncomplexed arene (or TNM)²³ or the generation of intermediates which do not result from the direct charge-transfer excitation of the EDA complexes.³³

When the CT excitation with the laser pulse was carried out under the conditions relevant to charge-transfer nitration as described in eq 7 (e.g., 0.2 M DMB and 0.1 M TNM in dichloromethane), an intense absorption in the visible region between 400

(32) See: Atherton, S. J. *J. Phys. Chem.* **1984**, *88*, 2840.

(33) Tamres, M.; Strong, R. L. In *Molecular Association*; Foster, R., Ed.; Academic: New York, 1979; Vol. 2, p 389.

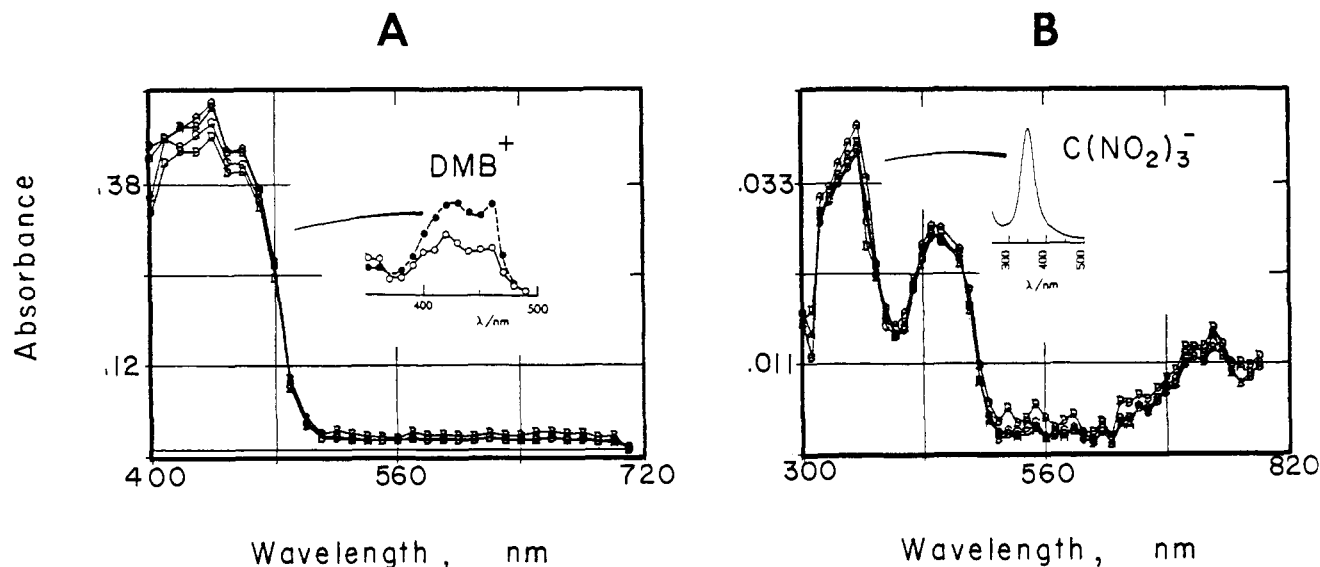


Figure 4. Transient absorption spectra from the 25-ps laser-pulse excitation at 532 nm of the EDA complex from (A) 0.2 M DMB and 0.15 M TNM and (B) 0.1 M DMB and 0.02 M TNM in CH₂Cl₂. The insets are the absorption spectrum of (A) DMB^{•+} from ref 34 and (B) C(NO₂)₃⁻ from the tetrabutylammonium salt.

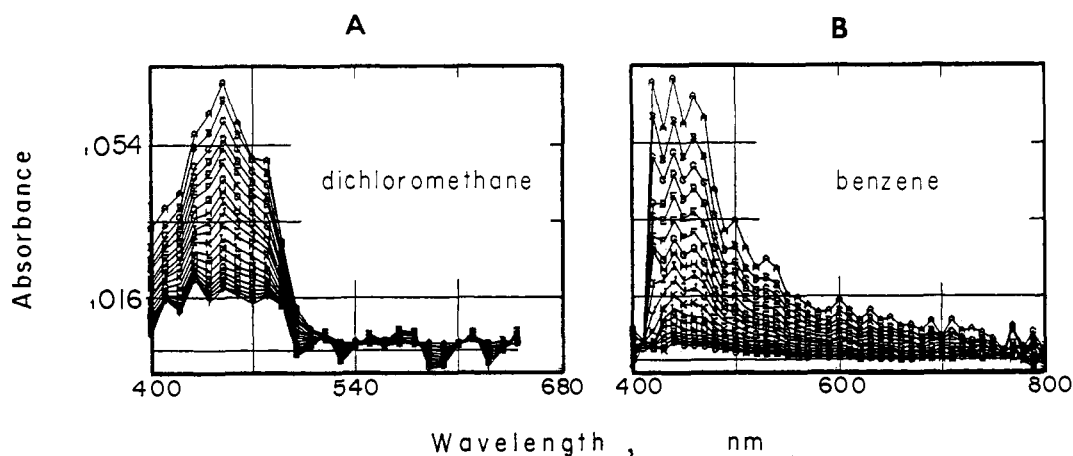
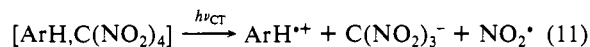


Figure 5. Time-resolved spectra of the transient cation radical EMP^{•+} in (A) dichloromethane and (B) benzene from the 25-ps CT excitation at 532 nm of 0.05 M EMP and 0.16 M TNM.

and 800 nm was observed immediately (<100 ns), and it persisted more or less unchanged for ~1 μs. Moreover, when solutions of the EDA complex prepared with increasing concentrations of dimethoxybenzene were pulsed, the enhancement of the absorbance at 440 nm followed Beer's law (see Experimental Section). The transient absorption band with λ_{max} = 440 nm in Figure 4A corresponded to the visible spectrum of the cation radical of 1,4-dimethoxybenzene, as shown by comparison in the inset with the absorption spectrum of the same species generated earlier by pulse radiolysis.³⁴ Any transient absorptions below 400 nm could only be observed with solutions of the EDA complex made up with minimum amounts of acceptor (e.g., 0.02 M TNM and 0.1 M DMB), owing to the interference from the tail of the tetranitromethane absorption.³⁵ Under these conditions a second absorption band with λ_{max} = 350 nm was clearly deduced (Figure 4B). It coincided with the spectrum of trinitromethide, and the identity was confirmed by spectral comparison with that of an authentic sample shown in the inset.³⁶ From the relative intensity of the absorption bands in Figure 4B for the aromatic cation radical [DMB^{•+}, ε = 9300 M⁻¹ cm⁻¹³⁴] and trinitromethide [C(NO₂)₃⁻,

ε = 14000 M⁻¹ cm⁻¹²⁶], we conclude that they are produced concomitantly and in equimolar amounts, i.e.



Nitrogen dioxide was not observed directly due to the weak and diffuse character of its absorption spectrum,^{37,38} and the presence in eq 11 was inferred from the stoichiometry. The absorption spectrum of the cation radical DMB^{•+} in dichloromethane (Figure 4A) was the same as that formed in *n*-hexane, benzene, acetonitrile, and methanol within the spectral resolution of ±10 nm.

The CT excitation of the EDA complexes of tetranitromethane and the dialkoxybenzenes with sidechains (MPA, EMP, and MPE) under similar conditions also led spontaneously to the corresponding aromatic cation radicals. As expected, all of these transient species absorbed strongly in the spectral region between 400 and 500 nm characterized for DMB^{•+} in Figure 4. A typical time-dependent change in the visible absorption resulting from the CT excitation of the EDA complex from the ethyl ester EMP is shown in Figure 5A. Although essentially the same spectrum was obtained in acetonitrile, a significant difference was observed in nonpolar solvents such as *n*-hexane and benzene. Figure 5B typically illustrates the pronounced tailing of the absorption band

(34) O'Neill, P.; Steenken, S.; Schulte-Frohlinde, D. *J. Phys. Chem.* **1975**, *79*, 2773.

(35) Rabani, J.; Mulac, W. A.; Matheson, M. S. *J. Phys. Chem.* **1972**, *76*, 26.

(36) Kaplan, L. A. In *Chemistry in Nitro and Nitroso Groups*; Fever, H., Ed.; Wiley: New York, 1970; Part 2, p 317.

(37) Hall, T. C., Jr.; Blacet, F. E. *J. Chem. Phys.* **1952**, *20*, 1745.

(38) Gillespie, G. D.; Khan, A. U. *J. Chem. Phys.* **1976**, *65*, 1624 and references therein.

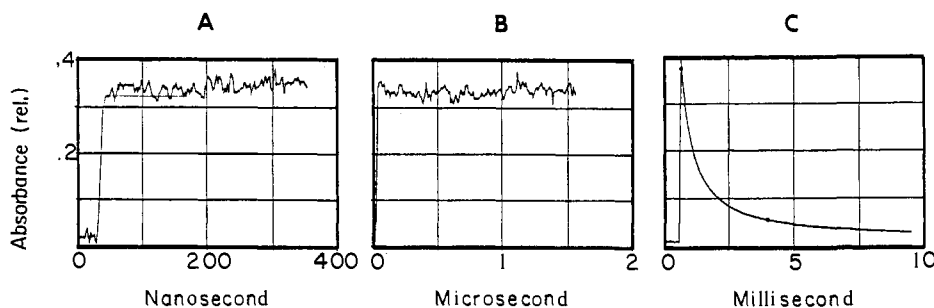


Figure 6. Decay behavior of the transient absorption at 460 nm of DMB^{**} in the (A) nanosecond, (B) microsecond, and (C) millisecond time regimes following the CT excitation at 532 nm of 0.05 M DMB and 0.17 M TNM in dichloromethane with a 25-ps laser pulse. The fit of the experimental decay to second-order kinetics is shown in part C by the fit to the computer-generated least-squares line (not discernible).

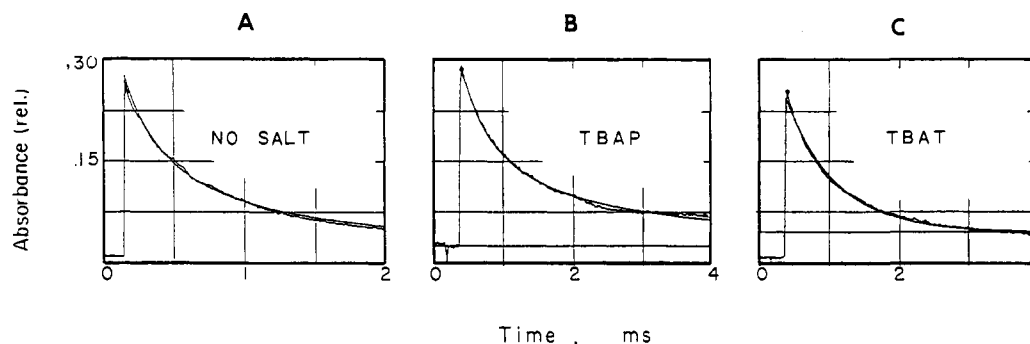
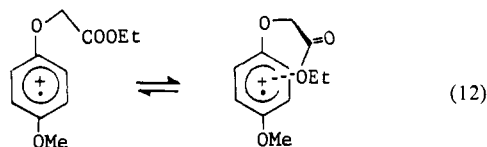


Figure 7. Salt effect on the decay of DMB^{**} followed at 440 nm in acetonitrile with (A) no additive, (B) 0.2 M TBAP, and (C) 0.01 M TBAT from the CT excitation of 0.05 M DMB and 0.25 M TNM. The smooth lines are then obtained from the computer-fitted least-squares treatment of the rate data for second-order kinetics.

of EMP^{**} to beyond 700 nm in benzene. Since the same spectral alteration was observed with the acid MPA and the alcohol MPE, but not with the parent DMB (*vide supra*), we tentatively attribute it to the solvent-dependent changes in the intramolecular association of the oxygen-containing side chain with the cationic arene center,³⁹ e.g.



Decay Kinetics of the Aromatic Cation Radicals Generated by CT Excitation. The transitory character of the various aromatic cation radicals following their spontaneous production by the charge-transfer excitation of the EDA complex was assessed by measuring the absorbance decrease at ~ 450 nm. Owing to the unique decay pattern of the aromatic cation radicals derived from DMB, MPA, EMP, and MPE, the behavior of each will be described separately.

A. The instantaneous rise of the 460-nm absorbance of DMB^{**} attendant upon the laser-pulse excitation of $[\text{DMB}, \text{TNM}]$ was followed by a quiescent period on the ns time scale and into the μs regime, as shown in Figure 6A,B under a typical set of conditions. The slower decay on the ms time scale is illustrated in Figure 6C; and the clean adherence to second-order kinetics is indicated by the excellent fit to the smooth line (not discernible) from the computer-fitted least-squares treatment of the decay profile.⁴⁰ The second-order rate constant $k_2 = 7 \times 10^3 \text{ A}^{-1} \text{ s}^{-1}$ in absorbance units (Table V) was applicable to the complete disappearance of DMB^{**} in dichloromethane, as established by

(39) Intramolecular solvation of the arene cation radical would be favored in media of low dielectric constant. Compare: Howell, J. O.; Goncalves, J. M.; Amatore, C.; Klasinc, L.; Wightman, R. M.; Kochi, J. K. *J. Am. Chem. Soc.* **1984**, *106*, 3968 and references therein.

(40) (a) The computer generated curves are based on the initial and final absorbances indicated with asterisks in the figures. (b) The kinetics orders are based on extensive trials and always represent unambiguous fits (with the exceptions noted).

Table V. The Decay Kinetics of DMB^{**} .^a Effect of Solvent and Added Salts

DMB (M)	TNM (M)	solvent	salt (M)	k_2^b	λ^c	int ^d
0.05	0.63	hexane		3.6×10^7	460	
0.05	0.08	benzene		2.9×10^5	460	
0.05	0.08	benzene	TBAP (0.01)	2.7×10^4	460	
0.05	0.08	benzene	TBAT (0.01)	2.2×10^5	450	
0.05	0.17	CH_2Cl_2		7.0×10^3	460	100
0.05	0.17	CH_2Cl_2		9.0×10^3	460	57
0.05	0.17	CH_2Cl_2		9.0×10^3	460	29
0.05	0.17	CH_2Cl_2	TBAP (0.2)	8.4×10^3	460	
0.05	0.17	CH_2Cl_2	TBAT (0.01)	8.8×10^3	470	
0.05	0.17	CH_3CN		1.0×10^4	440	
0.10	0.17	CH_3CN		9.1×10^3	440	
0.20	0.40	CH_3CN		9.5×10^3	440	
0.05	0.17	CH_3CN	TBAP (0.2)	2.1×10^4	440	

^a Following a 25-ps laser pulse at 532 nm. ^b Second-order rate constant in units of $\text{A}^{-1} \text{ s}^{-1}$. ^c Monitoring wavelength. ^d Laser intensity (relative).

the return of the 460-nm absorbance to the base line. Moreover the second-order rate constant which was essentially unchanged with the intensity of the laser pulse⁴¹ confirmed this kinetics analysis.

The decay of DMB^{**} also followed second-order kinetics in nonpolar solvents such as *n*-hexane and benzene. However, the rate of disappearance was highly solvent dependent, the second-order rate constants in hexane and benzene being 4 and 2 orders of magnitude, respectively, faster than that in dichloromethane (Table V). The decay of DMB^{**} in the highly polar acetonitrile generally followed second-order kinetics (Figure 7A), but it showed a slight deviation at high conversions ($>90\%$).^{40b} A leveling effect of the solvent is indicated by the magnitude of $k_2 = 9 \times 10^3 \text{ A}^{-1} \text{ s}^{-1}$ in acetonitrile, which is essentially that measured in dichloromethane.

The decay of DMB^{**} was subject to a minor salt effect with use of tetra-*n*-butylammonium trinitromethide (TBAT) and

(41) In relative units, see Experimental Section.

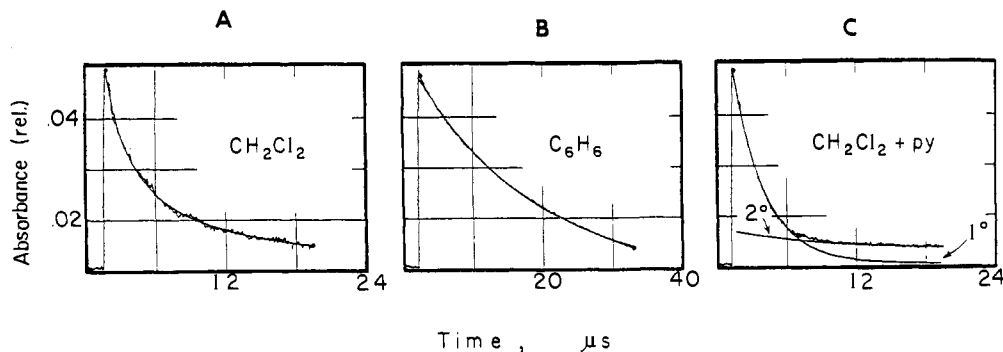


Figure 8. Solvent dependence of the decay kinetics of MPA^{•+} following the 532-nm excitation of 0.05 M MPA and 0.42 M TNM in (A) dichloromethane, (B) benzene, and (C) dichloromethane containing 0.1 M pyridine. The smooth lines are from the computer-generated least-squares treatment of the experimental data for (A) second-order, (B) first-order, and (C) initial first-order followed by second-order kinetics.

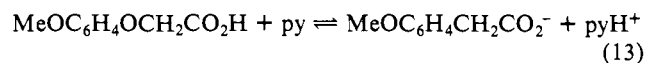
Table VI. Variation in the Decay Kinetics of MPA^{•+} with Solvent, Added Salt, and Pyridine Base^a

TNM (M)	solvent	additive	time scale	order ^b	rate constant ^c	λ ^d
0.17	benzene		10 μs	1°	1.5 × 10 ⁵	450
0.42	CH ₂ Cl ₂		~20 μs	2°	4.8 × 10 ⁶	460
0.20	CH ₂ Cl ₂	TBAP (0.2)	~1 ms	1°	1.9 × 10 ³	460
0.42	CH ₂ Cl ₂	pyridine (0.1)	1→6 μs	1°	3.6 × 10 ⁵	460
			6→20 μs	2°	4.3 × 10 ⁶	460
0.42	CH ₃ CN		>1 ms	1°	1.8 × 10 ³	460

^a Following 532-nm irradiation of 0.05 M MPA and TNM. ^b First-order (k_1) or second order (k_2) kinetics in the time scale indicated. ^c k_1 (s⁻¹) or k_2 (A⁻¹ s⁻¹), as indicated in column 5. ^d Monitoring wavelength (nm).

perchlorate (TBAP) as representatives of a common-ion and an unreactive additive, respectively.⁴² For example, the second-order rate constant k_2 in acetonitrile was unaffected by the presence of either 0.2 M TBAP or 0.01 M TBAT (Figure 7B,C). A slight negative salt effect was observed in a nonpolar solvent such as benzene (Table V).

B. The CT excitation of the TNM complex of the dialkoxyaromatic acid produced the cation radical MPA^{•+} which was persistent on the ns time scale. However the second-order rate constant of $k_2 = 5 \times 10^6 \text{ A}^{-1} \text{ s}^{-1}$ for the disappearance of MPA^{•+} in dichloromethane (Figure 8A) was ~3 orders of magnitude faster than that of DMB^{•+} under comparable conditions. Unlike the latter, however, the decay kinetics of MPA^{•+} was highly dependent on the solvent as well as on the additives. Thus the decay followed clean first-order behavior in nonpolar solvents such as benzene with $k_1 = 2 \times 10^5 \text{ s}^{-1}$ (see Table VI). The decay of MPA^{•+} also followed excellent first-order kinetics in dichloromethane containing 0.2 M TBAP (Figure 8B) but with a rate constant $k_1 = 2 \times 10^3 \text{ s}^{-1}$ which was 2 orders of magnitude slower than that obtained in benzene. More interestingly, the disappearance of MPA^{•+} in dichloromethane with pyridine deliberately added as a weak base,⁴³ i.e.



followed a biphasic decay pattern—an initial fast (within 1–5 μs) first-order component and a slower (within 10–20 μs) second-order decay. The first-order rate constant of $k_1 = 4 \times 10^5 \text{ s}^{-1}$ was comparable to that obtained in benzene; and the second-order rate constant with $k_2 = 4 \times 10^6 \text{ A}^{-1} \text{ s}^{-1}$ was essentially the same as that obtained in the absence of pyridine. The first-order rate constant $k_1 = 2 \times 10^3 \text{ s}^{-1}$ for the decay of MPA^{•+} in the polar acetonitrile was comparable to that obtained in dichloromethane with added TBAP.

Table VII. Solvent and Salt Effects on the Decay Kinetics of EMP^{•+}^a

solvent	salt (M)	time scale	order ^b	rate constant ^c	λ ^d
hexane		0.25 μs	1°	1.7 × 10 ⁶	450
		5→15 μs	1°	6.4 × 10 ⁴	
benzene		10→50 μs	1°	9.4 × 10 ⁴	450
		50→100 μs	1°	1.9 × 10 ⁴	450
benzene	TBAP (0.01)	200→500 μs	1°	6.3 × 10 ³	450
		0.5→2 ms	1°	1.6 × 10 ³	450
	TBAP (0.01)	200→500 μs	1°	8.7 × 10 ³	600
		0.5→2 ms	1°	2.3 × 10 ³	600
CH ₂ Cl ₂		0.2→2 ms	2°	4.4 × 10 ⁴	460
CH ₂ Cl ₂	TBAP (0.2)	0.2→4 ms	2°	3.4 × 10 ⁴	460
CH ₃ CN		0.2→4 ms	2°	4.0 × 10 ⁴	460

^a Generated from the 532-nm irradiation of 0.05 M EMP and 0.17 M TNM with a 25-ps laser pulse. ^b First-order (1°) or second-order (2°) kinetics in the time scale indicated. ^c k_1 (s⁻¹) or k_2 (A⁻¹ s⁻¹), as indicated in column 4. ^d Monitoring wavelength (nm).

Table VIII. Second-Order Decay of MPE^{•+} in Various Solvents^a

TNM (M)	solvent	λ	k_2 (A ⁻¹ s ⁻¹)
1.3	hexane	460	1.5 × 10 ⁶
0.17	benzene	450	1.0 × 10 ⁵
0.17	CH ₂ Cl ₂	460	2.5 × 10 ⁴
0.17	CH ₃ CN	460	3.0 × 10 ⁴

^a Following the 532 nm-irradiation of 0.05 M MPE with a 25-ps laser pulse. ^b Monitoring wavelength.

C. The decay pattern of the cation radical of ethyl 4-methoxyphenoxyacetate (EMP^{•+}) was more complicated than that of either DMB^{•+} or MPA^{•+} under comparable conditions. For example, the decay of EMP^{•+} in dichloromethane followed second-order kinetics with $k_2 = 4 \times 10^4$ which was intermediate between those for DMB^{•+} and MPA^{•+} generated similarly (vide supra). The presence of 0.2 M TBAP diminished the second-order rate constant slightly (Table VII). In nonpolar solvents such as *n*-hexane and benzene the decay was biphasic. Thus the kinetics analysis of the initial fast fall-off of the absorbance revealed a first-order process (k_1), and it was followed by a slower decay (k_1') which also obeyed first-order kinetics (Table VII). Both first-order rate constants were depressed by the presence of added TBAP (0.01 M). Since the absorption spectrum of EMP^{•+} in benzene showed a low-energy tail beyond 700 nm (vide supra), the analysis was also carried out at a pair of different wavelengths. The kinetics behavior of the absorbance decay at 450 and 600 nm was identical, and the associated first-order rate constants were comparable.

D. The disappearance of the cation radical MPE^{•+} from *p*-methoxyphenoxyethanol was reminiscent of behavior of the parent cation DMB^{•+} described above. Thus the decay cleanly followed second-order kinetics to high conversions (>95%) in all the solvents. Moreover the second-order rate constants in Table VIII are comparable to those obtained for DMB^{•+} under similar conditions.

(42) Masnovi, J. M.; Levine, A.; Kochi, J. K. *Chem. Phys. Lett.* **1985**, *119*, 351.

(43) Perrin, D. D.; Dempsey, B.; Serjeant, E. P. *pK_a Prediction of Organic Acids and Bases*; Chapman and Hall: New York, 1981.

Table IX. Quantum Yields (Steady-State) for the Charge-Transfer Nitration of DMB in Various Solvents^a

DMB (M)	TNM (M)	solvent	duration (h)	$\Phi_{\text{-DMB}}^b$	Φ_{N}^c
0.10	0.67	CH ₂ Cl ₂	12	0.40	0.31
0.15	0.75	CH ₃ CN	20	0.40	0.35
0.10	0.33	benzene	4	0.66	0.46
0.10	0.33	C ₆ H ₆ /TBAP	10	0.50	0.41
0.05	0.50	hexane	8 ^{1/2}	0.43	0.22

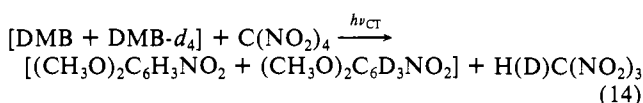
^aCT irradiation at 520 ± 5 nm. ^bFor the disappearance of DMB. ^cFor the production of 2,4-dimethoxynitrobenzene.

Quantum Yields for Charge-Transfer Nitration. The photoefficiency of the charge-transfer nitration of 1,4-dimethoxybenzene was measured with a Reinecke actinometer⁴⁴ and carried out with monochromatic light by passing the output from a 500-W high-pressure mercury lamp through a 520-nm interference filter (10-nm band pass). The photolysate containing 2,5-dimethoxynitrobenzene and unreacted DMB was analyzed by quantitative gas chromatography with internal standards. The quantum yields for CT nitration were determined as Φ_{N} from the formation of 2,5-dimethoxynitrobenzene and as $\Phi_{\text{-DMB}}$ from the disappearance of the arene (see Experimental Section).

The quantum yields Φ_{N} and $\Phi_{\text{-DMB}}$ in Table IX are comparable, and both are consistently high in polar (acetonitrile) and in nonpolar solvents (hexane). Furthermore they are unaffected by the presence of added salt (i.e., 0.01 M TBAP).

Deuterium Kinetic Isotope Effect in Charge-Transfer Nitration. The kinetic isotope effect for charge-transfer nitration was evaluated by the direct competition between the protio 1,4-(CH₃O)₂C₆H₄ and the deuterio 1,4-(CH₃O)₂C₆D₄. The specific deuteration of the arene ring positions was achieved by multiple isotopic exchange of DMB in trifluoroacetic acid-*d*₁.⁴⁵ The exchange yielded material that was >99% isotopically pure by mass spectral analysis.

From the GC-MS analysis of the reaction mixture for the disappearance of the isotopic 1,4-dimethoxybenzenes as well as the appearance of the isotopic 2,5-dimethoxynitrobenzenes, i.e.



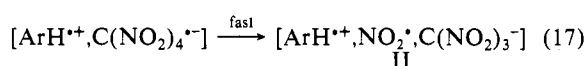
at both high and low conversions (see Experimental Section), we conclude the kinetic isotope effect to be $k_{\text{H}}/k_{\text{D}} = 1.02 \pm 0.02$.

Discussion

The direct observation of the reactive intermediates by the use of time-resolved spectroscopy and fast kinetics allows the course of charge-transfer nitration to be charted in some detail. We proceed in the analysis from the mechanistic context originally presented in Scheme I, namely, the evolution and metamorphosis of arene ion radical pairs.

I. Spontaneous Evolution of the Ion Radical Pair [ArH^{•+},NO₂^{•-}] by Charge-Transfer Excitation. Picosecond time-resolved spectroscopy has defined the relevant photophysical and photochemical processes associated with the charge-transfer excitation of an arene complex such as anthracene with tetrannitromethane.¹⁵ As applied to the aromatic ethers ArH examined in this study, the formation of the pertinent ion radical pair by charge-transfer excitation is summarized in Scheme III.

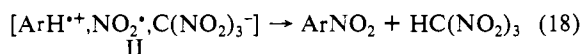
Scheme III



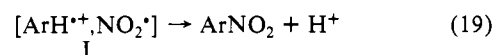
All the experimental observations with aromatic ethers and tetranitromethane indeed coincide with the formulation in Scheme III. Thus the exposure of ArH to a nitrating agent such as TNM as in Figure 1 leads immediately to the EDA complex in eq 15. These binary complexes are present in low steady-state concentrations owing to the limited magnitudes of *K* as measured by the Benesi-Hildebrand method (Figure 3 and Table IV). Activation of the EDA complex by the specific irradiation of the CT band (Figure 1) results in a photoinduced electron transfer (eq 16) in accord with Mulliken theory.²³ The irreversible fragmentation following the electron attachment to TNM leads to the ion radical pair II in eq 17 (see Figure 4). The measured quantum yield of $\Phi \approx 0.5$ in Table IX is similar to that ($\Phi \approx 0.7$) previously obtained for anthracene in Scheme II.⁴⁶ Such high quantum yields relate directly to the efficiency of ion radical pair production in eq 17 relative to energy wastage by back-electron transfer in eq 16. Moreover the short lifetime (<3 ps) of C(NO₂)₄^{•-} ensures that ArH^{•+} and NO₂^{•-} are born as an intimate ion radical pair, initially trapped within the solvent cage, since this time scale obviates any competition from diffusional processes.^{15,47,48}

Charge-transfer excitation thus provides the experimental means to generate the intimate ion radical pair [ArH^{•+},NO₂^{•-}] for Scheme I in sufficient concentrations and in a discrete electronic state as well as geometric configuration. Coupled with the observation of the fast kinetics allowed by the use of laser-flash photolytic techniques, we now focus on the pathways by which the ion radical pair collapses to nitration products.

II. Transformation of the Ion Radical Pair [ArH^{•+},NO₂^{•-}] to Nitration Products. The excellent material balance obtained in charge-transfer nitration (Table III) demands that the ion radical pair II in Scheme III proceeds quantitatively to the nitration products according to the stoichiometry



Such a transformation must occur spontaneously with no discrimination among the reactive intermediates to accord with the absence of a deuterium kinetic isotope effect in eq 14.⁴⁹ The latter is not consistent with the collapse of II as an ion pair [ArH^{•+},C(NO₂)₃^{•-}] by proton transfer to the very weakly basic trinitromethide (deliberately added as the salt TBAT) exerts essentially no influence on either the course (Table III) or the kinetics (Table V). Accordingly we consider the trinitromethide to be merely an innocuous bystander insofar as the conversion of the ion radical pair II in eq 18 is concerned.⁵⁰ It follows that the disappearance of the arene ion radical must be directly related to its interaction with NO₂^{•-}, viz.⁵¹



Indeed such cation radicals have been prepared from various arenes by other experimental methods,⁵⁴ especially electrochemical ox-

(46) Masnovi, J. M.; Kochi, J. K. *J. Org. Chem.* **1985**, *50*, 5245.

(47) Bielski, B. H. J.; Allen, A. O. *J. Phys. Chem.* **1967**, *71*, 4544.

(48) Chaudhuri, S. A.; Asmus, K. D. *J. Phys. Chem.* **1972**, *76*, 26. See also: Glover, D. *J. Tetrahedron* **1963**, *19* (Suppl. I), 219.

(49) No deuterium isotope effect is observed in the electron detachment from arenes to produce ArH^{•+}.

(50) Trinitromethide serves as the base in the subsequent deprotonation of the Wheland intermediate (see eq 21), especially in nonpolar media.

(51) Arene cation radicals are known to form π -dimer cations, especially with electron-rich arenes.⁵² However, the similarity of the absorption spectrum of DMB^{•+} in Figure 4, A and B, and that reported by O'Neill et al.³⁴ indicate that we are dealing primarily with the monomeric species. The subsequent kinetics analysis is carried out on this basis.⁵³ See also Masnovi et al.³⁰

(52) (a) Edlund, O.; Kinell, P.-O.; Lund, A.; Shimizu, A. *J. Chem. Phys.* **1967**, *46*, 3679. (b) Badger, B.; Brocklehurst, B. *Trans. Faraday Soc.* **1969**, *65*, 2576, 2582, 2588. (c) Kira, A.; Arai, S.; Imamura, M. *J. Phys. Chem.* **1972**, *76*, 119. (d) Lau, W.; Kochi, J. K. *J. Org. Chem.* **1986**, *51*, 1801.

(53) For the comparative reactivities of an ArH^{•+} and its π -dimer, see: Masnovi, J. M.; Kochi, J. K. *J. Phys. Chem.* **1987**, *91*, 1878.

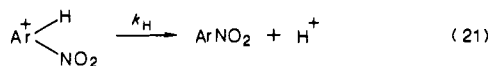
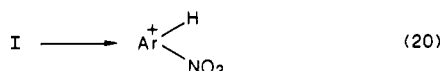
(54) Bard, A. J.; Ledwith, A.; Shine, H. J. *Adv. Phys. Org. Chem.* **1976**, *14*, 155.

(44) Wegner, E. E.; Adamson, A. W. *J. Am. Chem. Soc.* **1966**, *88*, 394.

(45) Cf. Lau, W.; Kochi, J. K. *J. Am. Chem. Soc.* **1984**, *106*, 7100.

idation.⁵⁵ The arene cation radicals of the type generated in Table III are weak Brønsted acids, but they are highly susceptible to nuclear addition,^{6,55,56} e.g.

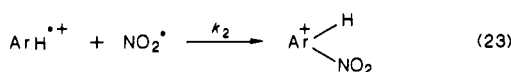
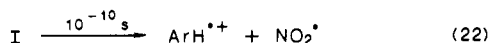
Scheme IV



The σ -adduct in eq 20 is the Wheland intermediate in electrophilic nitration, which is known to show no deuterium kinetic isotope effect for k_H upon deprotonation in eq 21.^{7,57,58} According to Scheme IV, the formation of the various isomeric Wheland intermediates will occur from the collapse of the ion radical pair in eq 20. Consequently the isomer distributions in the nitration products relate directly to the relative rates of addition to the various nuclear positions provided that it is irreversible and/or the adduct deprotonates rapidly. Thus the strong correlation observed between the spin densities at the various nuclear positions of ArH⁺ and the isomeric product distribution in aromatic nitration^{4,5,7,59} bears directly on the mechanics of such an ion radical pair collapse to the Wheland intermediate.

Although the Wheland intermediate in Scheme IV has not been separately observed in our experiments,⁶⁰ the time-resolved spectral changes of the cation radical ArH⁺ do provide insight as to how it is formed. Thus the relatively long lifetimes of the arene cation radicals in Figures 5–8 are sufficient to allow diffusive separation of the ion radical pair I to ArH⁺ and NO₂[•] as essentially “free” species.⁶² The second-order process with the rate constant k_2 for the disappearance of DMB^{•+} in Table V then represents the “re”combination of these separated species to form the Wheland intermediate, i.e.

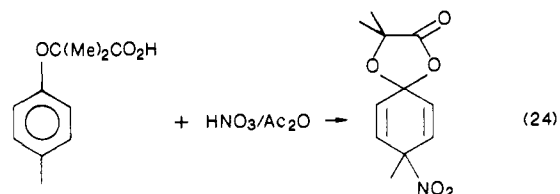
Scheme V



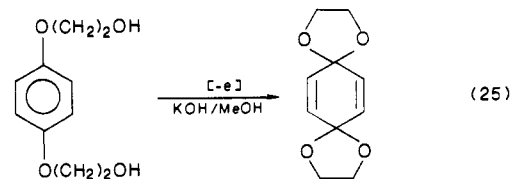
We attribute the strong solvent dependence of k_2 largely to the stabilization of ArH⁺ by solvation, since it decreases with increasing solvent polarity in the following order: hexane > benzene > dichloromethane. The slight negative salt effect on k_2 also accords with this conclusion. [In a related system, the rate of combination of a neutral aromatic radical (hydranthryl) with NO₂[•] was shown to be both solvent and salt independent.⁶²]

Since the common-ion salt TBAT has no effect on the charge-transfer nitration of DMB in Table V, we concluded that trinitromethide is not a sufficiently strong nucleophile to intercept the associated cation radical DMB^{•+} in a process that would be tantamount to ion pair collapse of II. However, it has been shown in electrophilic nitration that the Wheland intermediate can be

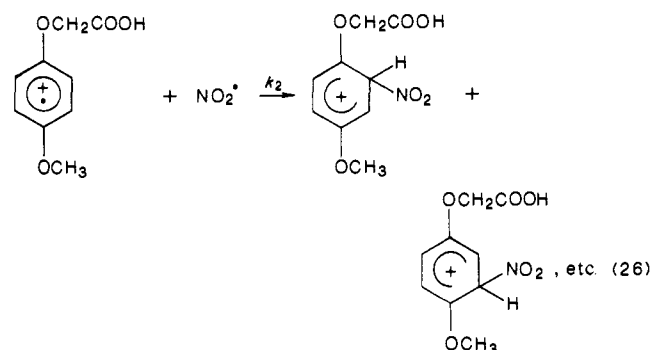
efficiently captured by a built-in nucleophile, usually a carboxylic acid, and the nitration product isolated as an *ipso* adduct, e.g.⁶³



Moreover the intramolecular capture of arene cation radicals generated by electrochemical oxidation has been demonstrated.⁶⁴



Accordingly we examined the effects of built-in nucleophiles on the reactive intermediates from 4-methoxyphenoxyacetic acid (MPA), since both electrophilic and charge-transfer lead to the same mixture of isomeric ArNO₂ in excellent yields, as shown in Tables II and III, respectively. The observed second-order kinetics for the disappearance of MPA^{•+} in dichloromethane (Table VI) reflect the formation of the isomeric σ -adducts, i.e.⁶⁵



in accord with Scheme V (eq 23). However, when pyridine is present in the dichloromethane solution to deprotonate the carboxylic acid (see eq 13), the decay of the cation radical shows biphasic kinetics,⁶⁶ i.e., an initial first-order falloff followed by a second-order rate profile. The fast first-order decay with $k_1 = 4 \times 10^5 \text{ s}^{-1}$ represents the intramolecular capture of the cationic arene center by a pendant carboxylate nucleophile (see eq 28b).⁶⁷ The competing second-order rate process, with a value of $k_2 = 4 \times 10^6 \text{ M}^{-1} \text{ s}^{-1}$, which is the same as that obtained in the absence of pyridine (vide supra), must therefore be associated with the residual conjugate acid MPA^{•+}, as in eq 26. The composite mechanism is schematically summarized in Scheme VI.⁶⁹ In a

(55) For a recent review, see: Yoshida, K. *Electrooxidation in Organic Chemistry*; Wiley: New York, 1984.

(56) (a) Parker, W. D.; Ebersson, L. *Tetrahedron Lett.* **1969**, 2839, 2843. (b) Schlesener, C. J.; Kochi, J. K. *J. Org. Chem.* **1984**, *49*, 3142. (c) Kochi, J. K.; Tang, R. T.; Bernath, T. *J. Am. Chem. Soc.* **1973**, *95*, 7114.

(57) Melander, L. *Arkiv Kemi* **1950**, *2*, 211. Halvarson, K.; Melander, L. *Arkiv Kemi* **1957**, *11*, 77. See also: Melander, L. *Isotope Effects on Reaction Rates*; Ronald Press: New York, 1960.

(58) See also: (a) Lauer, W. M.; Noland, W. E. *J. Am. Chem. Soc.* **1953**, *75*, 3689. (b) Olah, G. A.; Kuhn, S. J.; Flood, S. H. *J. Am. Chem. Soc.* **1961**, *83*, 4571. (c) Beug, M.; James, L. L. *J. Am. Chem. Soc.* **1968**, *90*, 2105. (d) For a review see Schofield.⁷

(59) Fukuzumi, S.; Kochi, J. K. *J. Am. Chem. Soc.* **1981**, *103*, 7240.

(60) The Wheland intermediate or arenium ion is expected to show absorption in the 300–400-nm region,⁶¹ which is unfortunately obscured in our studies.

(61) Koptuyg, V. A. *Contemporary Problems in Carbonium Ion Chemistry III*; Springer Verlag: New York, 1984; p 96 ff.

(62) Masnovi, J. M.; Kochi, J. K. *J. Am. Chem. Soc.* **1985**, *107*, 7880.

(63) Fischer, A.; Fyles, D. L.; Henderson, G. N. *J. Chem. Soc., Chem. Commun.* **1980**, 513. See also: Fischer, A.; Leonard, D. R. A.; Roderer, R. *Can. J. Chem.* **1979**, *57*, 2527.

(64) (a) Magaretha, P.; Tissot, P. *Helv. Chim. Acta* **1975**, *58*, 933. (b) Nilsson, A.; Palmquist, U.; Patterson, T.; Ronlan, A. *J. Chem. Soc., Perkin Trans. I* **1978**, 708.

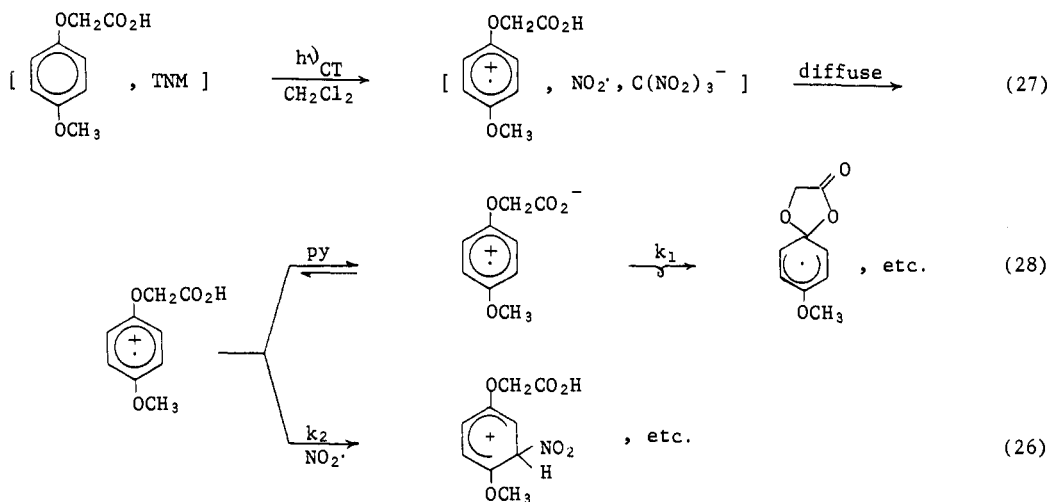
(65) Since k_2 for MPA^{•+} is $\sim 10^3$ times faster than that for DMB^{•+}, it is unlikely that the zwitterion (cf. eq 30) is involved in eq 26.

(66) The absorption spectra of the cation radical and the zwitterion are expected to be very similar if not the same.

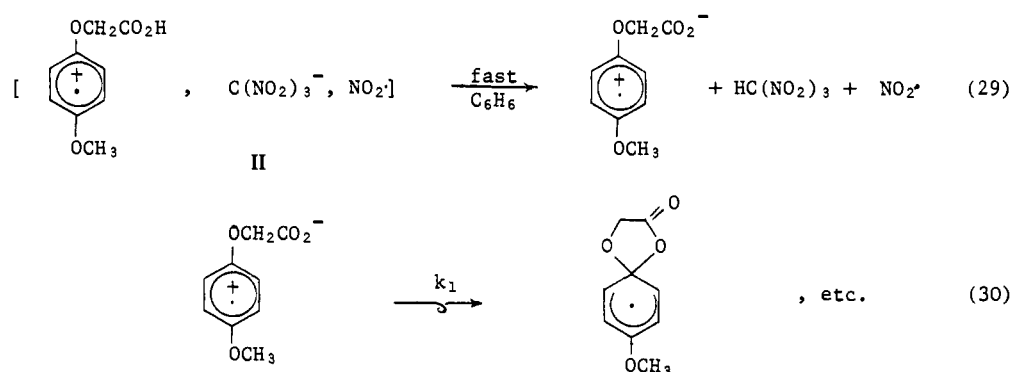
(67) Intramolecular capture may occur at either the ipso position as shown or the ortho position. In either case, the absorption spectrum of the resulting cyclohexadienyl radical is likely to be similar to that of the hydroxide adduct to DMB^{•+} in ref 34. Since $\lambda_{\text{max}} \approx 300 \text{ nm}$ for these adduct radicals,⁶⁸ they cannot be observed in our system.

(68) (a) Jordan, J. E.; Pratt, D. W.; Wood, D. E. *J. Am. Chem. Soc.* **1974**, *96*, 5588. (b) Effio, A.; Griller, D.; Ingold, K. U.; Scaiano, J. C.; Sheng, S. *J. Am. Chem. Soc.* **1980**, *102*, 6063. (c) Bunce, N. J.; Ingold, K. U.; Landers, J. P.; Luszytk, J.; Scaiano, J. C. *J. Am. Chem. Soc.* **1985**, *107*, 5464.

Scheme VI



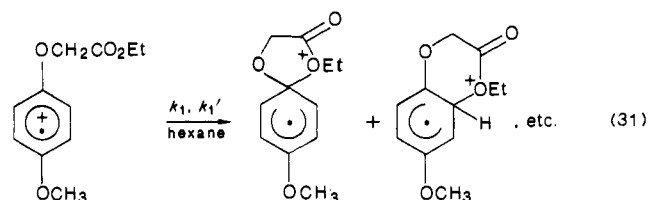
Scheme VII



nonpolar solvent such as benzene, the same first-order rate process with $k_1 = 2 \times 10^5 \text{ s}^{-1}$ now accounts for all of the decay of $\text{MPA}^{\cdot+}$ (see Table IV). Under these conditions, the deprotonation of the cation radical $\text{MPA}^{\cdot+}$ by the trinitromethide counteranion is quite likely to occur within the ion radical pair II prior to diffusive separation into the medium of low dielectric constant,⁷⁰ i.e. see Scheme VII. The intramolecular neutralization of the cationic charge in $\text{MPA}^{\cdot+}$ to form the zwitterion in eq 29 provides the driving force for deprotonation.⁷² The first-order kinetics observed in acetonitrile and in dichloromethane containing 0.2 M TBAP suggests that the deprotonation of $\text{MPA}^{\cdot+}$ is even possible with a large excess of weak bases such as MeCN and ClO_4^- .⁷⁰ The value of $k_1 = 2 \times 10^3 \text{ s}^{-1}$, which is two orders of magnitude slower than that obtained in benzene, may reflect a degree of stabilization of the zwitterion by polar and ionic media.

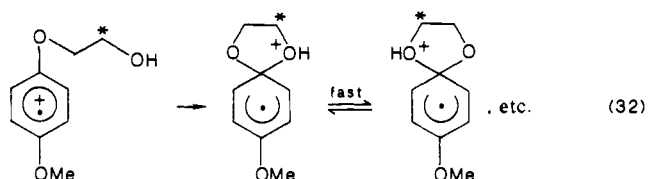
In the absence of an ionizable side chain as in the ester derivative, the cation radical $\text{EMP}^{\cdot+}$ behaves much like the parent $\text{DMB}^{\cdot+}$ in solvents such as dichloromethane and acetonitrile. The second-order rate constants in Table VII thus reflect the bimolecular reaction of $\text{EMP}^{\cdot+}$ with NO_2^{\cdot} to afford the Wheland intermediate, as in Scheme V and eq 26. However, in nonpolar solvents (hexane and benzene) the absorption spectrum of $\text{EMP}^{\cdot+}$ has a low-energy tail that is absent in $\text{DMB}^{\cdot+}$ (compare Figure 5) and attributed to intramolecular association. Indeed the ex-

planation presented in eq 12 could relate to the first-order kinetics reported in Table VII, e.g.⁶⁷



In all the solvents, the charge-transfer nitration of ethyl 4-methoxyphenoxyacetate yields only 2-nitro and 3-nitro derivatives of EMP with the ester functionality intact.⁷³

Intramolecular trapping of the cation radical by the side chains in $\text{MPA}^{\cdot+}$ (eq 30) and $\text{EMP}^{\cdot+}$ (eq 31) does not occur in the ethyl alcohol derivative MPE. Thus the decay kinetics of MPE⁺ in Table VIII are the same as those observed in the parent $\text{DMB}^{\cdot+}$ (compare Table V). In principle, the intramolecular collapse of MPE⁺ would produce a symmetrical intermediate and lead to methylene scrambling in the side chain, i.e.



The absence of such scrambling during the electrophilic and

(69) It is possible that the zwitterion in eq 28a is also directly formed by a concurrent CT excitation of the TNM complex with the conjugate base of MPA.

(70) The conversion of ArH to $\text{ArH}^{\cdot+}$ is accompanied by substantial increase in acidity.⁷¹

(71) See, e.g.: (a) Bordwell, F. G.; Bausch, M. J. *J. Am. Chem. Soc.* **1986**, *108*, 2473. (b) Schlesener, C. J.; Amatore, C.; Kochi, J. K. *J. Am. Chem. Soc.* **1984**, *106*, 7472.

(72) For the solvent effect on the acidity of nitroform, see: Lewis, E. S. *Chemistry of Nitro and Nitroso Groups, Supplement F*; Patai, S., Ed.; Wiley: New York, 1982; Part 2.

(73) The evolution of nitro products from NO_2 and the cyclohexadienyl radicals formed in eq 28, 30, and 31 is undefined at this juncture. However, it must accord with the invariance of the isomer distributions from MPA, EMP, and MPE in different solvents (see Experimental Section). Further studies of such a homolytic process are in progress.

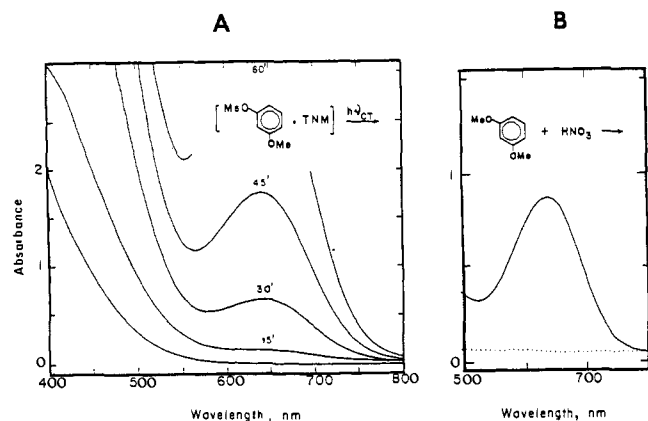
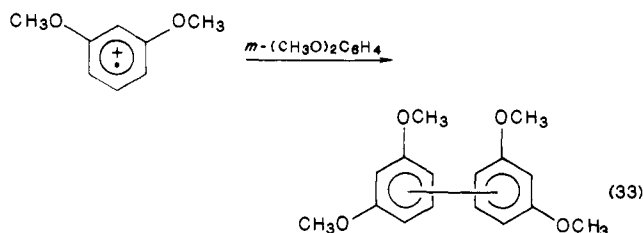


Figure 9. (A) Appearance of the blue species accompanying the CT excitation of 0.03 M *m*-dimethoxybenzene and 0.7 M TNM in dichloromethane for 0, 15, 30, 45, and 60 min. (B) Absorption spectrum (after 1000-fold dilution) of the blue species obtained from the nitration of 0.3 M *m*-dimethoxybenzene with 1 equiv of nitric acid in glacial acetic acid.

charge-transfer nitration of the isotopically labeled alcohol in Table III is thus in accord with the kinetics results. The ethyl alcohol side chain of MPE exerts negligible influence on nitration, and the collapse of the cation radical MPE^{•+} with NO₂[•] is similar to that given in eq 26.

Direct Comparison of Electrophilic and Charge-Transfer Nitrations. Aromatic nitration via the ion radical pair I in eq 19 proceeds with high efficiency when it is induced by the charge-transfer excitation of arene-TNM complexes. Furthermore the yields and isomeric distributions among the nitration products in Table III are strikingly akin to those obtained under the more conventional electrophilic conditions in Table II. One can conclude from these observations that intermediates leading to electrophilic nitration are similar to, if not the same as, those derived by charge-transfer nitration. Indeed the parallel behavior extends even to those arenes in which significant amounts of byproducts are formed. For example, the direct nitration of *m*-dimethoxybenzene is reported to produce 2,4-dimethoxynitrobenzene in only poor yields (~30%).⁷⁴ In addition, we observe an unusual blue coloration to develop rapidly during the electrophilic nitration of *m*-dimethoxybenzene. The same intense blue color occurs with *m*-dimethoxybenzene and TNM, but only upon the deliberate exposure of the EDA complex to CT irradiation, as shown by the spectral comparison in Figure 9. Among the dimethoxybenzenes, the meta isomer is unique in that it is the only one to develop an intense (blue) coloration upon electrophilic and/or charge-transfer nitration. The subsequent chromatography of the highly colored reaction mixture from electrophilic nitration yields significant amounts of dimethoxyphenyl dimers (vide infra), which are known to derive from the cation radical by arene coupling,^{54,55,75,76} i.e.

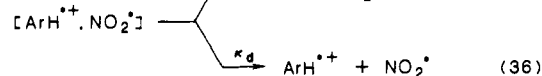
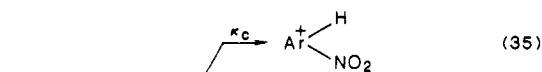
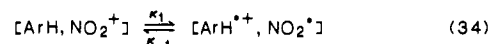


We observe similar results with 2,6-dimethoxytoluene and 1,3,5-trimethoxybenzene (see Experimental Section).

Comments on Electrophilic Nitration. The observations described above underscore the strong similarity between electrophilic and charge-transfer nitration of aromatic ethers, with regard to

both the nitration products and the diaryl byproducts. Since the latter is symptomatic of arene cation radicals, the parallelism does extend to some reactive intermediates in common. As such, the most economical formulation for electrophilic nitration would also include a pathway that is common to charge-transfer nitration, namely, via the ion radical pair I, as originally presented in Scheme I (eq 1-3).⁷⁷ This mechanism differs from the conventional formulation in which the [ArH,NO₂⁺] pair in eq 1 is directly converted to the Wheland intermediate in a single step, rather than via the ion radical pair I. Previous studies have established the strong similarity in the activation barriers (i.e., energetics) for these two processes.^{59,80} Accordingly let us consider the problem in an alternative framework, namely, the lifetime of the ion radical pair. At one extreme of a very short lifetime, the ion radical pair is tantamount to the transition state for the concerted one-step process. At the other extreme of a very long lifetime, the ion radical pair is manifested by its diffusive separation. Scheme VIII presents this construct in a kinetics context.⁸¹

Scheme VIII



According to Scheme VIII the efficient collapse of the ion radical pair to the Wheland intermediate is represented by $\kappa_c \gg \kappa_d$. On this basis the time scale of the "concerted" process is limited by the diffusional correlation times of $<10^{-11}$ s.⁸² The extent to which $\kappa_c \ll \kappa_d$ allows side reactions to compete is a result of the diffusive separation of ArH^{•+} and NO₂[•]. Our experiments with aromatic ethers clearly belong in the latter category since the evolution of nitration products takes place in the $\mu\text{s}/\text{ms}$ time regime. Nonetheless the diffusive recombination of ArH^{•+} and NO₂[•] pairs with the rate constant k_2 can occur in eq 23 with very high efficiency. The competition from diffusion is represented by the intra- and intermolecular trapping of ArH^{•+} in eq 30/31 and eq 33, respectively. The ion radical pair formulation thus represents a unifying theme for electrophilic and charge-transfer nitration. Indeed it can account for all of the diverse experimental observations of aromatic ethers with little or no ambiguity. However, we hasten to add the caveat that these aromatic donors may not be truly representative of less reactive arenes. We hope that laser-flash studies at the ps/ns time resolutions will provide the means to examine CT transients with shorter lifetimes required for the further test of Scheme I.

Experimental Section

Materials. Veratrole, 1,3- and 1,4-dimethoxybenzene (Eastman), and 1,3,5-trimethoxybenzene (Aldrich) were used as received. 2,6-Dimethoxytoluene (Aldrich) and 3,4-dimethoxyphenylacetonitrile (Aldrich) were repurified by sublimation. 3,5-Dimethoxyphenylacetonitrile (Eastman)

(77) Note that all electrophilic nitrating agents are equivalent to electron acceptors such as tetranitromethane in their charge-transfer properties.⁷⁸ Moreover TNM is capable of thermal nitration of electron-rich arenes.⁷⁹

(78) Fukuzumi, S.; Kochi, J. K. *J. Org. Chem.* **1981**, *46*, 4116.

(79) (a) Schmidt, E.; Fischer, H. *Ber. Dtsch. Chem. Ges* **1920**, *53*, 1529. (b) Allsop, S.; Allsop, F.; Kenner, J. *J. Chem. Soc.* **1923**, *123*, 2314. (c) Schmidt, E.; Schumacher, R. *Ber. Dtsch. Chem. Ges* **1921**, *54*, 1414. (d) Anderson, A. G.; Scotoni, R.; Cowles, E. J.; Fritz, G. G. *J. Org. Chem.* **1957**, *22*, 1193. (e) Hafner, K.; Moritz, K. *L. Justus Liebigs Ann.* **1962**, *656*, 40. (f) Reid, D. H.; Stafford, W. H.; Stafford, W. L. *J. Chem. Soc.* **1958**, 1118. (g) Chaudhuri, J. N.; Basu, S. *J. Chem. Soc.* **1959**, 3085. (h) Bruce, T. C.; Gregory, M. J.; Walter, S. L. *J. Am. Chem. Soc.* **1968**, *90*, 1612. (i) Isaacs, N. S.; Abed, O. H. *Tetrahedron Lett.* **1982**, *23*, 2799. (j) Seltzer, S.; Lam, E.; Packer, L. *J. Am. Chem. Soc.* **1982**, *104*, 6470.

(80) See also: Lau, W.; Kochi, J. K. *J. Am. Chem. Soc.* **1986**, *108*, 6720.

(81) See also: Schofield, J. pp 107 ff.

(82) Even shorter times are possible depending on the interaction energy in the ion radical pair.^{62,83}

(83) (a) Fukuzumi, S.; Kochi, J. K. *J. Phys. Chem.* **1980**, *84*, 608, 2246, 2254. (b) Dewar, M. J. S.; Kuhn, D. R. *J. Am. Chem. Soc.* **1986**, *108*, 551.

(74) Loudon, J. D.; Ogg, J. *J. Chem. Soc.* **1955**, 739.

(75) McKillop, A.; Turrell, A. G.; Young, D. W.; Taylor, E. C. *J. Am. Chem. Soc.* **1980**, *102*, 6504.

(76) Musgrave, O. C. *Chem. Rev.* **1969**, *69*, 499.

was purified by crystallization from aqueous methanol. Tetranitromethane was prepared by nitration of acetic anhydride.⁸⁴ Glacial acetic acid and fuming nitric acid were from Mallinckrodt. Hexane (EM Science), benzene (Fisher), dichloromethane (Fisher), and acetonitrile (Burdick and Jackson) were spectral grade solvents. Tetra-*n*-butylammonium trinitromethide was prepared as reported earlier.⁶² *p*-Methoxyphenol (Matheson, Coleman & Bell) and ethyl chloroacetate (Eastman) for the preparation of ethyl *p*-methoxyphenoxyacetate were used without further purification. 1,4-Dimethoxybenzene-*d*₄ was prepared by refluxing it in a 1:1 (by vol) mixture of trifluoroacetic anhydride and D₂O overnight.⁴⁵ The procedure was repeated 3 times to obtain 99% isotopic incorporation by mass spectral analysis. A pure sample of 1,4-DMB-*d*₄ was obtained by sublimation. Lithium aluminum deuteride was obtained from Chemical Dynamics, and Reinecke salt from Aldrich. The remaining aromatic ethers were synthesized as follows.

Ethyl 4-Methoxyphenoxyacetate. A mixture of *p*-methoxyphenol (0.1 mol), ethyl chloroacetate (0.1 mol, 10.6 mL), sodium iodide (0.1 mol, 15 g), and anhydrous potassium carbonate (0.2 mol, 28 g) was refluxed in anhydrous acetone (80 mL) for 12 h.⁸⁵ The mixture was cooled and filtered. The solid residue was washed with methylene chloride, and the washings were combined with the filtrate. The solution was evaporated and the crude product was obtained as a golden yellow oil. It was purified by vacuum distillation to give colorless oil. Ethyl 4-methoxyphenoxyacetate: yield 82%; bp 102–105 °C (0.01 mmHg); IR (neat) 3051 (w), 2984 (s), 2937 (s), 2836 (s), 1757 (s, C=O), 1737 (sh), 1595 (w), 1509 (s), 1465 (s), 1443 (s), 1379 (m), 1285 (s), 1212 (s), 1085 (s), 1034 (s), 828 (s), 722 (m) cm⁻¹; ¹H NMR (CDCl₃) 6.83 (s, 4 H, aromatic), 4.55 (s, 2 H, OCH₂CO), 4.25 (q, 2 H, OCH₂CH₃, *J* = 7.1 Hz), 3.75 (s, 3 H, OCH₃), 1.28 (t, 3 H, OCH₂CH₃, *J* = 7.1 Hz) ppm; ¹³C NMR (CDCl₃) 169.1 (C=O), 154.4 (C-4), 152.0 (C-1), 115.8 and 114.6 (C-2, C-3, C-5, and C-6), 66.3 (OCH₂CO), 61.2 (OCH₂CH₃), 55.5 (OCH₃), 14.0 (OCH₂CH₃) ppm; MS (70 eV) 210 (M⁺, 42), 182 (20), 137 (39), 124 (86), 123 (58), 109 (20), 107 (28), 105 (13), 95 (43), 92 (35), 81 (20), 80 (23), 79 (36), 78 (26), 77 (100), 65 (52), 64 (39).

4-Methoxyphenoxyacetic Acid. This phenoxyacetic acid was obtained by the hydrolysis of the ethyl ester (0.1 mol) in 200 mL of 10% aqueous sodium hydroxide. After the mixture was refluxed for 2 h, it was cooled and then acidified with concentrated HCl whereupon the acid crystallized as a colorless solid. It was filtered and recrystallized from a hot methanol-water mixture. 4-Methoxyphenoxyacetic acid: yield 78%; mp 108–110 °C (lit.⁸⁶ mp 110–112 °C); ¹H NMR (CDCl₃) 7.89 (br s, 1 H, OH), 6.85 (s, 4 H, aromatic), 4.62 (s, 2 H, OCH₂CO), 3.76 (s, 3 H, OCH₃) ppm; IR (KBr) 3000–2500 (br, OH), 1737 (s, C=O), 1709 (s), 1625 (w), 1510 (s), 1465 (s), 1428 (s), 1379 (w), 1325 (m), 1292 (s), 1271 (s), 1222 (s), 1116 (m), 1090 (s), 1036 (s), 905 (m), 826 (s) cm⁻¹; ¹³C NMR (CDCl₃) 174.6 (C=O), 154.7 (C-4), 151.6 (C-1), 115.8 and 114.8 (C-2, C-3, C-5, and C-6), 65.7 (OCH₂CO), 55.7 (OCH₃) ppm.

2'-(4-Methoxyphenoxy)ethanol. In a three-necked flask fitted with a reflux condenser and a pressure adjusted dropping funnel, lithium aluminum hydride (0.7 g, 0.018 mol) was suspended in anhydrous ether (20 mL) and the suspension was cooled in an ice bath. A solution of ethyl 4-methoxyphenoxyacetate (2.6 g, 0.012 mol) in anhydrous ether (20 mL) was added dropwise with magnetic stirring. After the addition of the ester, the mixture was refluxed for 1 h and cooled in an ice bath. Excess lithium aluminum hydride was destroyed by careful addition of ethyl acetate followed by methanol. The mixture was acidified with concentrated HCl, and the ether layer was separated and dried over anhydrous MgSO₄. Evaporation of ether yielded the crude alcohol as a colorless crystalline solid. It was recrystallized from an ether-hexane mixture. Yield 82%; mp 68–70 °C; IR (KBr) 3298 (br, OH), 2954 (s), 2930 (s), 2870 (w), 2835 (w), 1870 (w), 1639 (w), 1512 (s), 1462 (m), 1444 (m), 1378 (m), 1294 (s), 1245 (s), 1177 (w), 1114 (s), 1094 (s), 1053 (s), 1033 (s), 932 (m), 922 (m), 891 (m), 827 (s) cm⁻¹; ¹H NMR (CDCl₃) 6.84 (s, 4 H, aromatic), 3.99 (m, 4 H, OCH₂CH₂OH), 3.76 (s, 3 H, OCH₃), 2.29 (br s, 1 H, OH) ppm; ¹³C NMR (CDCl₃) 153.9 (C-4), 152.6 (C-1), 115.4 and 114.6 (C-2, C-3, C-5, and C-6), 69.8 (OCH₂CH₂), 61.4 (OCH₂CH₂), 55.5 (OCH₃) ppm; MS (70 eV) 169 (3), 168 (29, M⁺), 124 (100), 109 (91), 81 (18), 77 (13), 64 (14), 63 (13), 53 (13). 2'-(4-Methoxyphenoxy)ethanol-1',1'-*d*₂ was prepared by the same procedure with lithium aluminum deuteride. The crude product was recrystallized from an ether-hexane mixture to yield colorless crystals of the pure dideuterio alcohol. Yield 78%; mp 68–70 °C; IR (KBr) 3297 (br, s, OH), 2953 (m), 2926 (m), 2867 (w), 2836 (w), 2109 (m), 1868 (w), 1513 (s), 1456 (m), 1292 (s), 1243 (s), 1177 (s), 1114 (m), 1054 (s), 1032 (s), 977 (s), 895 (m), 826 (s), 693 (m) cm⁻¹; ¹H NMR (CDCl₃)

6.84 (s, 4 H, aromatic), 4.01 (s, 2 H, OCH₂), 3.76 (s, 3 H, OCH₃), 2.29 (br s, 1 H, OH) ppm; ¹³C NMR (CDCl₃) 153.9 (C-4), 152.6 (C-1), 115.4 and 114.5 (C-2, C-3, C-5, and C-6), 69.7 (OCH₂CD₂), 60.6 (quintet, OCH₂CD₂OH, *J*_{C-D} = 22 Hz), 55.6 (OCH₃) ppm; MS (70 eV) 170 (43, M⁺), 125 (14), 124 (100), 110 (19), 109 (84), 95 (10), 81 (17), 77 (12), 63 (12), 53 (10).

Instrumentation. The UV-vis spectra were recorded on a Hewlett-Packard 8450A diode-array spectrometer. A Nicolet 10DX FT spectrometer was used to record all IR spectra. NMR spectra were recorded on a JEOL FX90Q spectrometer operating at 90 MHz for ¹H and 22.5 MHz for ¹³C. Proton chemical shifts are reported in ppm downfield from a Me₄Si internal standard. Carbon-13 chemical shifts are reported in ppm, and either the resonance for Me₄Si (δ_C = 0 ppm) or the center of the multiplet resonance for the solvent (e.g., CDCl₃ = 77.0 ppm) was taken as reference. The NMR data are reported in the following format: chemical shift in ppm (multiplicity, number of protons, assignment of proton, coupling constant in Hz). The gas chromatographic analyses were performed on a Hewlett-Packard 5790A chromatograph with a 12.5 M SE 30 (cross-linked methylsilicone) capillary column. The GC-MS analyses were carried out on a Hewlett-Packard 5890 chromatograph interfaced to a HP5970 mass spectrometer (EI, 70 eV). Melting points were determined on a MEL-TEMP (Laboratory Devices) apparatus and are uncorrected. Photochemical irradiations were performed with a focussed beam from either a 500 W Osram (HBO-2L2) high pressure Hg or a 1000 W Hanovia (977B0010) Hg-Xe lamp. The light was passed through an IR water filter coupled to a Corning CS-3-72 (425 nm) or CS-3-70 (500 nm) glass cutoff filter.

Time-resolved differential absorption spectra in the microsecond time scale were obtained on a laser-flash system. It utilized the 532-nm second harmonic 10-ns pulses from a Quantel YG 481 Nd:YAG laser, which was monitored with a 150 W Xenon lamp. A SPEX minimate monochromator, Hamamatsu R928 NM photomultiplier tube, and either a Tektronix R7912 digitizer or a Biomation 8100 waveform recorder were used for the probe assembly.⁸⁷ Signals were digitized, averaged, and interfaced with a Digital Equipment PDP 11/70 computer for analysis.⁸⁸ For the differential absorption spectra and decay kinetics in the ns time scale the 532-nm second harmonic from a mode-locked Nd:YAG (Quantel) laser with a 200-ps pulse was used. The concentration of the arene cation radical DMB^{•+} can be determined in the time-resolved spectra in Figure 4 (e.g., ϵ at 460 nm in 9540 M⁻¹ cm⁻¹). The absorbance at 450 nm with the variation of DMB (M) was 0.015 (0.01), 0.030 (0.02), 0.057 (0.04), 0.090 (0.06), and 0.115 (0.08) upon the CT irradiation of the EDA complex from solutions containing 0.16 M TNM.

For the disappearance of the arene cation radicals, in each experiment 10 to 30 shots were averaged to obtain the decay curves. The reaction order of the decay was established by a linear least-squares computer fit of the observed decrease of the absorbance (*A*) with time as a function of either ln *A* or *A*⁻¹ for first or second order, respectively. For more complicated decays, a fitting routine was utilized to extract the rate constants sequentially by determining the rate of the slower component initially.⁶²

Electrophilic Nitration of Aromatic Ethers with Nitric Acid. The electrophilic nitration of the aromatic ethers was carried out according to Clark with 1 equiv of nitric acid in glacial acetic acid.²⁰ In a typical experiment, a solution of nitric acid (fuming) (0.4 mL, 9.5 mmol) in glacial acetic acid (2 mL) previously cooled to 0 °C in an ice bath was added slowly to a well-stirred solution of the substrate (9.5 mmol) in glacial acetic acid (2 mL) at 0 °C. The mixture was stirred at 0 °C for 1.5 h and then warmed to room temperature and stirred for an additional 2 h. The reaction mixture was worked up by adding ether (~50 mL) and washing the ethereal solution with ice cold water. The ethereal layer was dried over anhydrous MgSO₄, and the ether was removed in vacuo with a rotary evaporator. The crude product was obtained either as a yellow viscous oil (in the case of *p*-methoxyphenoxyethanol, methyl *p*-methoxyphenoxyacetate, and 1,4-dimethoxybenzene) or as a yellow crystalline solid (as in the case of *p*-methoxyphenoxyacetic acid).

Since the nitration of *m*-dimethoxybenzene and its congeners differed from the other aromatic ethers, the procedure is described separately. A solution of fuming nitric acid (0.3 mL, 7 mmol) in glacial acetic acid (2 mL) was added dropwise to a stirred ice cold solution of 1,3-DMB (0.69 g, 5 mmol). The solution turned intense bluish-green instantaneously upon the addition of the nitrating agent. A small aliquot of this solution was diluted (~1000-fold) with acetic acid, and the electronic spectrum of the bluish-green solution was recorded (Figure 9B). The remaining solution was stirred at room temperature for 1.5 h and then poured onto ice. Upon neutralization with saturated NaHCO₃ solution, the reaction mixture turned deep red. Extraction with ether followed by CH₂Cl₂ and

(84) Liang, P. *Organic Syntheses*; Wiley: New York, 1955; Collect. Vol. III, p 803.

(85) Brettell, R. *J. Chem. Soc.* **1956**, 1891.

(86) Koelsch, C. F. *J. Am. Chem. Soc.* **1931**, 53, 304.

(87) Atherton, S. J. *J. Phys. Chem.* **1984**, 88, 2840.

(88) Foyt, D. C. *J. Comput. Chem.* **1981**, 5, 49.

evaporation of the combined organic extracts (after drying over anhydrous MgSO₄) yielded a reddish-brown slurry (0.65 g). The crude reaction mixture was analyzed by GC and ¹H NMR, which indicated the formation of two major products. The mixture was passed through a short column of alumina and eluted with ether. Pure 2,4-dimethoxynitrobenzene was obtained as a colorless crystalline solid: mp 72–74 °C (lit.⁸⁹ mp 74 °C); ¹H NMR (CDCl₃) 7.98 (d, 1 H, H-6, *J* = 10 Hz), 6.54 (d, 1 H, H-3, *J* = 2.4 Hz), 6.48 (dd, 1 H, H-5, *J* = 10, 2.3 Hz), 3.94 (s, 3 H, 2-OCH₃), 3.88 (s, 3 H, 4-OCH₃) ppm; MS (70 eV) 183 (M⁺, 74), 153 (25), 136 (100), 125 (33), 122 (16), 110 (17), 107 (35), 95 (15), 93 (17), 92 (38), 79 (43), 78 (12), 77 (66), 69 (25), 66 (23), 63 (47), 62 (18). In a separate experiment, the reaction was carried out in acetic acid-*d*₄ and the course followed by ¹H NMR spectroscopy as follows. To a solution of 1,3-DMB (10 μL, 0.07 mmol) in acetic acid-*d*₄ (0.5 mL), fuming HNO₃ was added at 0 °C and the ¹H NMR spectrum of the resulting dark bluish-green solution was recorded with CH₂Cl₂ as the internal standard (0.15 mmol). The ¹H NMR spectrum indicated the complete disappearance of the starting material and the formation of 2,4-dimethoxynitrobenzene (0.04 mmol, 57%). The other major product that was formed in the reaction was most likely a dimer of 1,3-dimethoxybenzene based on the GC-MS analysis which showed peaks at *m/z* 274 (17), 273 (100), 258 (18), 230 (25), 172 (20), 151 (22), 138 (51), 137 (34), 107 (34), 69 (30), 63 (25).

2,6-Dimethoxytoluene (DMT). To an ice-cold solution of 2,6-dimethoxytoluene (0.76 g, 5 mmol) in glacial acetic acid (3 mL) was added dropwise the nitrating agent consisting of fuming nitric acid (0.3 mL, 7 mmol) in glacial acetic acid. The solution turned deep blue and the electronic spectrum of the solution was recorded after dilution with glacial acetic acid (approximately 1000-fold dilution) (λ_{max} = 600 nm). The reaction mixture was stirred at room temperature for 1.5 h, poured onto ice, neutralized with solid NaHCO₃, and extracted with CH₂Cl₂. Removal of CH₂Cl₂ after drying the extracts over anhydrous MgSO₄ yielded a reddish-brown oil (0.6 g). ¹H NMR and GC analysis indicated two major products and several other minor products. Filtration of the ethereal solution of the crude product through a short column of neutral alumina followed by elution with ether yielded a yellow solution. Evaporation of solvent yielded 2,6-dimethoxy-3-nitrotoluene as a yellow viscous oil (0.1 g, 12%). Structure assignment was based on the ¹H NMR spectrum which showed a pair of doublets in the aromatic region with *J* = 9 Hz corresponding to two aromatic hydrogens mutually ortho. ¹H NMR (CDCl₃) 7.88 (d, 1 H, H-4, *J* = 9 Hz), 6.66 (d, 1 H, H-5, *J* = 9 Hz), 3.91 (s, 3 H, 2-OMe), 3.87 (s, 3 H, 6-OMe), 2.18 (s, 3 H, 1-CH₃) ppm; MS (70 eV) 197 (M⁺, 71), 167 (28), 150 (100), 121 (37), 108 (22), 107 (23), 106 (37), 93 (26), 91 (60), 79 (23), 78 (35), 77 (50), 65 (53), 63 (23), 52 (22). The other major product present in the crude reaction mixture is likely to be a product of dimerization of 2,6-dimethoxytoluene. It had the following MS (70 eV): 303 (24), 302 (20), 301 (100), 286 (55), 257 (33), 255 (23), 242 (26), 204 (23), 165 (29), 163 (18), 152 (51), 151 (27), 149 (20), 121 (47), 108 (20), 93 (51), 91 (26), 83 (27), 77 (45), 65 (53).

1,3,5-Trimethoxybenzene (TMB). Nitration of 1,3,5-trimethoxybenzene (0.21 g, 1.2 mmol) was carried out as described in the case of 2,6-dimethoxytoluene. Upon the addition of the nitrating agent, a deep blue color developed (λ_{max} = 608 nm). After the mixture was stirred at room temperature for 1.5 h, it was worked up as described above. Pure 2,4,6-trimethoxynitrobenzene (0.05 g, 18%) was isolated by filtering the crude product through a short column of alumina and eluting with ether. The product had mp 152 °C (lit.⁹⁰ mp 152 °C) (yellow crystals). ¹H NMR (CDCl₃) 6.12 (s, 2 H, H-3,5), 3.85 (s, 6 H, CH₃O-2,6), 3.84 (s, 3 H, CH₃O-4) ppm; MS (70 eV) 213 (M⁺, 100), 183 (73), 155 (64), 140 (37), 137 (49), 125 (49), 123 (26), 122 (37), 109 (39), 107 (19), 81 (18), 79 (26), 77 (37), 66 (31), 65 (17), 59 (53), 53 (52).

Charge-Transfer Nitration of Aromatic Ethers with Tetranitromethane. 1,4-Dimethoxybenzene. The EDA complexes formed from 1,4-dimethoxybenzene and excess TNM in various solvents, with and without added salts, were irradiated with a focussed beam from the 500 W mercury lamp. The irradiations were performed in a 1 cm quartz cell immersed in a Pyrex dewar filled with water to maintain the temperature at 18 ± 2 °C. A Corning cutoff filter (λ < 425 nm, CS 3-72) was used to ensure the irradiation of only the CT band. In cases where tetrabutylammonium trinitromethide (TBAT) was used as a common ion salt, a Corning cutoff filter (λ < 510 nm, CS 3-69) was used. Reactions were followed spectrophotometrically by the disappearance of the CT band. Reactions were complete within 4–8 h depending on the solvent and the added salt (Table X). After the reaction was complete, the solvent and excess TNM were removed in vacuo and the crude product was analyzed by ¹H NMR spectroscopy with either hexamethylbenzene or CH₂Cl₂ as the internal

Table X. Charge-Transfer Nitration of 1,4-Dimethoxybenzene with Tetranitromethane^a

solvent	DMB (M)	TNM (M)	salt (M)	duration (h)	yield ^b (%)
hexane	0.06	0.13		3.5	85
benzene	0.06	0.28		3.25	95
benzene	0.06	0.28	TBAP (0.01) ^c	4	95
benzene ^d	0.06	0.95	TBAT (0.01)	12	95
CH ₂ Cl ₂	0.03	0.67		4	93
CH ₂ Cl ₂	0.05	0.42	TBAP (0.2)	3	95
CH ₂ Cl ₂ ^a	0.06	1.11	TBAT (0.01)	12	92
CH ₃ CN	0.03	0.67		5.5	100
CH ₃ CN	0.05	0.42	TBAP (0.2)	6.5	100

^aBy irradiation with λ > 425 nm, unless indicated otherwise. ^bBy ¹H NMR analysis with C₆Me₆ or CH₂Cl₂ as internal standard. ^cSaturated solution. ^dIrradiation at λ > 510 nm.

Table XI. Charge-Transfer Nitration of 4-Methoxyphenoxyacetic Acid with Tetranitromethane^a

solvent	MPA (M)	TNM (M)	salt (M)	duration (h)	yield ^b (%)
benzene	0.05	0.55		7	90
CH ₂ Cl ₂	0.06	0.83		4	98
CH ₂ Cl ₂	0.17	0.45	TBAP (0.2)	6	100 ^c
CH ₃ CN	0.11	0.42		6	100 ^c

^aBy irradiation with λ > 425 nm. ^bIsolated yield. ^cBy ¹H NMR integration of both isomers.

standard. The identity of 2,5-dimethoxynitrobenzene was confirmed by comparison of the IR, ¹H and ¹³C NMR, and MS spectra with those of an authentic sample.²¹ In all the solvents except hexane, the CT nitration was clean and yielded 2,5-dimethoxynitrobenzene as the only product in almost quantitative yield.

Photolysis in hexane yielded 2,5-dimethoxynitrobenzene as the major product (85%) together with small amounts of another product which was insoluble in ether, methylene chloride, and chloroform, but soluble in acetone. It was not characterized further.

4-Methoxyphenoxyacetic Acid. A mixture of MPA and TNM in 3 mL of solvent was irradiated in a 1-cm quartz cell immersed in a Pyrex dewar and thermostated at 18 ± 2 °C. A focussed beam from a 500 W mercury lamp passing through a Corning cutoff filter (CS 3-72, λ < 425 nm) was used to irradiate the CT band. The reaction was followed spectrophotometrically by the disappearance of the CT band. When the CT nitration was carried out in benzene and methylene chloride, the product precipitated during the course of the reaction. After the reaction was complete, the excess TNM and solvent were removed and the product was isolated as a yellow crystalline solid. The ¹H NMR spectrum of the crude product in acetone-*d*₆ indicated the formation of a mixture of 2-nitro- and 3-nitro-4-methoxyphenoxyacetic acid in approximately 3:7 ratio, respectively. The ratio of the isomers was the same in benzene, CH₂Cl₂, and acetonitrile (Table XI). The isomers were not separated. The identity of the products was confirmed by comparison with the authentic sample obtained by the direct nitration of *p*-methoxyphenoxyacetic acid in acetic acid with fuming nitric acid.²⁰ 4-Methoxy-2-nitrophenoxyacetic acid: ¹H NMR (CD₃COCD₃) 7.13 (m, 1 H, H-3), 6.97 (m, 2 H, H-5,6), 4.55 (s, 2 H, CH₂), 3.55 (s, 3 H, OCH₃) ppm. 4-Methoxy-3-nitrophenoxyacetic acid: ¹H NMR (CD₃COCD₃) 7.13 (m, 1 H, H-2), 6.97 (m, 2 H, H-5,6), 4.49 (s, 2 H, CH₂), 3.62 (s, 3 H, OCH₃) ppm; IR (KBr) 2793 (br, OH), 1747 (s, C=O), 1712 (s), 1626 (w), 1581 (m), 1532 and 1366 (s, NO₂), 1454 (s), 1431 (s), 1312 (m), 1272 (s), 1227 (s), 1073 (s), 1017 (s), 923 (s), 872 (s), 823 (s), and 813 (s) cm⁻¹. For GC-MS analysis, the mixture of 2-nitro- and 3-nitro-4-methoxyphenoxyacetic acid was converted into the corresponding methyl ester. The esterification was performed in 1-mmol scale in a diazomethane generator as described in the literature.⁹¹ Methyl 4-methoxy-2-nitrophenoxyacetate: MS (70 eV) 242 (10, M⁺ + 1), 241 (92, M⁺), 196 (11, M + 1 - NO₂), 195 (100, M⁺ - NO₂), 168 (17), 153 (25), 152 (46), 124 (49), 124 (46), 110 (25), 109 (35), 108 (20), 107 (29), 93 (23), 80 (22), 79 (59), 77 (25), 69 (50), 63 (50). Methyl 4-methoxy-3-nitrophenoxyacetate: MS (70 eV) 242 (12, M⁺ + 1), 241 (100, M⁺), 168 (43, M⁺ - CH₂COOCH₃), 123 (22), 121 (22), 107 (70), 79 (52), 78 (21), 77 (23), 76 (42), 73 (25), 66 (17), 65 (12), 63 (25). The course of the charge-transfer nitration of MPA in benzene was followed periodically to determine whether any unstable intermediates were present. A solution of 4-methoxyphenoxyacetic acid (18 mg, 0.1

(89) Loudon, J. D.; Ogg, J. J. *Chem. Soc.* **1955**, 739.

(90) Kampouris, E. M. J. *Chem. Soc. C* **1967**, 2568.

(91) Black, T. H. *Aldrichimica Acta* **1983**, 16, 3.

Table XII. Charge-Transfer Nitration of Ethyl 4-Methoxyphenoxyacetate with Tetranitromethane^a

solvent	EMP (M)	TNM (M)	salt (M)	duration (h)	yield ^b (%)
benzene	0.11	0.55		6	80 ^c
CH ₂ Cl ₂	0.11	0.55		7.5	93
CH ₂ Cl ₂	0.15	0.40	TBAP (0.2)	6.25	95
CH ₃ CN	0.11	0.40		4	100

^a By irradiation with $\lambda > 425$ nm. ^b Based on ¹H NMR analysis. ^c Isolated yield.

mmol) and TNM (130 μ L, 1 mmol) in benzene-*d*₆ (2 mL) was irradiated with a focussed beam from a 1000-W Hg lamp equipped with a water filter and a Corning 425-nm cutoff filter. Irradiation was performed in a Pyrex tube immersed in ice-cold water. Upon photolysis the solution turned cloudy after 15 min and remained cloudy throughout the photolysis. The reaction was followed by ¹H NMR spectroscopy by withdrawing a small aliquot of the photolysate. Before recording the ¹H NMR spectrum a few drops of acetone-*d*₆ were added to clarify the solution. The ¹H NMR spectrum of the photolysate at various intervals indicated the gradual disappearance of the starting material and formation of 2-nitro and 3-nitro isomers as the sole products. The methoxy and the methylene resonances of the starting material and the products were sufficiently separated to obtain good integration and the relative amounts were calculated by using the resonance of CH₂Cl₂ as the internal standard. The results—serially given as time, MPA (%), 2-NO₂ product (%), 3-NO₂ product (%), 2NO₂/3NO₂, mass balance (%)—were the following: 30, 44, 17, 38, 3/7, 100; 60, 19, 19, 56, 2.6/7.4, 94; 90, 10, 21, 59, 2.7/7.3, 90; 120, 0, 25, 66, 2.8/7.2, 91.

Ethyl 4-Methoxyphenoxyacetate. Photolysis of the EDA complex from EMP and excess TNM in various solvents was performed as described above for 4-methoxyphenoxyacetic acid. The crude product consisted of ethyl 2-nitro- and 3-nitro-4-methoxyphenoxyacetate in 3:7 ratio, respectively, as indicated by ¹H NMR analysis. The ratio of the two isomers remained unchanged in all the solvents used (Table XII). The products were identified by comparison with authentic samples obtained by the direct nitration of ethyl 4-methoxyphenoxyacetate in acetic acid with fuming nitric acid.²⁰ Nitric acid nitration also yielded the 2-nitro and 3-nitro isomers in the same ratio (3:7) as the photonitration. The isomers were separated by column chromatography on a silica gel column with ether-petroleum ether as eluent (20:80 vol %). Ethyl 4-methoxy-2-nitrophenoxyacetate: yellow viscous oil; IR (neat) 3086 (m), 2984 (s), 2844 (s), 1755 (s, C=O), 1534 (s, NO₂), 1501 (s), 1443 (s), 1354 (s, NO₂), 1291 (s, 1209 (s), 1092 (s), 1059 (s), 1037 (s), 917 (m), 859 (m), and 811 (s) cm⁻¹; ¹H NMR (CDCl₃) 7.37 (m, 1 H, H-3), 7.04 (m, 2 H, H-5,6), 4.70 (s, 2 H, OCH₂), 4.25 (q, 2 H, CH₂CH₃, *J* = 7.1 Hz), 3.82 (s, 3 H, OCH₃), 1.28 (t, 3 H, CH₂CH₃, *J* = 7.1 Hz) ppm; ¹³C NMR (CDCl₃) 168.0 (C=O), 154.0 (C-4), 145.3 (C-1), 140.6 (C-2), 120.3 (C-6), 117.9 (C-5), 109.8 (C-3), 67.7 (OCH₂), 61.4 (CH₂CH₃), 55.8 (OCH₃), 13.9 (CH₂CH₃) ppm; MS (70 eV) 255 (37, M⁺), 182 (17), 181 (100), 153 (17), 152 (32), 139 (16), 136 (13), 124 (45), 123 (26), 111 (13), 110 (17), 109 (25), 108 (18), 107 (25), 95 (16), 84 (13), 93 (19), 80 (11), 79 (52), 69 (27), 65 (13). Ethyl 4-methoxy-3-nitrophenoxyacetate: yellow viscous oil; IR (neat) 3086 (w), 2984 (s), 2941 (s), 2843 (m), 1755 (s, C=O), 1532 (s, NO₂), 1501 (s), 1443 (s), 1356 (s, NO₂), 1278 (s), 1204 (s), 1095 (s), 1069 (s), 1019 (s), 915 (s), 813 (s), 734 (s) cm⁻¹; ¹H NMR (CDCl₃) 7.40 (d, 1 H, H-2, *J* = 2.80 Hz), 7.20 (dd, 1 H, H-6, *J* = 2.80, 104 Hz), 7.03 (d, 1 H, H-5, *J* = 10.4 Hz), 4.62 (s, 2 H, OCH₂), 4.27 (q, 2 H, CH₂CH₃, *J* = 7.1 Hz), 3.92 (s, 3 H, OCH₃), 1.30 (t, 2 H, CH₂CH₃, *J* = 7.1 Hz) ppm; ¹³C NMR (CDCl₃) 168 (C=O), 150.8 (C-4), 148.0 (C-1), 139.2 (C-3), 121.6 (C-5), 114.9 (C-6), 111.4 (C-2), 66.0 (OCH₂), 61.4 (OCH₂CH₃), 56.9 (OCH₃), 39 (CH₂CH₃) ppm; MS (70 eV) 256 (13), 255 (100, M⁺), 182 (25), 168 (27), 123 (26), 122 (22), 121 (18), 93 (14), 79 (50), 78 (19), 77 (14), 76 (37), 75 (13), 66 (13), 65 (15), 63 (26). The structural assignments based on the ¹H NMR chemical shifts were supported by the shift reagent as follows. Tris(6,6,7,7,8,8,8-heptafluoro-2,2-dimethyl-3,5-octanedionate)europium [Eu(fod)₃] was used as the shift reagent. In a typical experiment, 35 mg of the substrate in 300 μ L of CDCl₃ was used for the ¹H NMR spectrum. A stock solution of the shift reagent was prepared by dissolving 125 mg of the reagent in 1 mL of CDCl₃. It was added in 25- μ L increments and the spectra were recorded. In both isomers, with the addition of increasing amounts of the shift reagent the methylene protons (OCH₂COO) were shifted downfield more rapidly relative to the methoxy protons (OCH₃). This indicated that the shift reagent preferentially complexed with the OCH₂COO group rather than the OCH₃ group. (The shift reagent may be chelated by the carbonyl oxygen and the oxygen attached to the aromatic ring.) Addition of the shift reagent resolved the ¹H NMR spectrum of the aromatic region into

Table XIII. Charge-Transfer Nitration of Methoxyphenoxyethanol with Tetranitromethane^a

solvent	MPE (M)	TNM (M)	duration (h)	yield ^b (%)
CH ₂ Cl ₂	0.10	0.28	5	85
CH ₃ CN	0.10	0.28	5	96
CH ₂ Cl ₂	0.20 ^c	0.27	6	96
CH ₃ CN	0.20 ^c	0.27	6	96

^a By irradiation with $\lambda > 425$ nm. ^b By ¹H NMR analysis with C₆Me₆ internal standard. ^c MPE-*d*₂.

an ABX pattern which facilitated the assignment of the individual aromatic hydrogens based on the coupling constants. Finally the change in the chemical shift of the individual protons is plotted against the change in the chemical shift of the methylene protons. Each plot consisted of 10 points. A linear fitting with correlation coefficient of 0.99 was obtained by the least-squares method for each plot. The slope (ρ) of the lines for the 2-nitro and the 3-nitro isomers is given below with respect to the slope of the methylene protons being unity. Ethyl 2-nitro-4-methoxyphenoxyacetate: H-3, H-5, H-6, OCH₃; ρ = 0.06, 0.10, 0.30, 0.03, respectively. Ethyl 3-nitro-4-methoxyphenoxyacetate: H-2, H-5, H-6, OCH₃; ρ = 0.40, 0.08, 0.35, 0.05, respectively. We took the site of complexation to be the OCH₂COO group in both isomers. In the 2-nitro isomer H-6 shifted much more downfield than H-3 and H-5, whereas in the 3-nitro isomer both H-2 and H-6 were shifted much more than H-5.

2'-(4-Methoxyphenoxy)ethanol. Photolysis of the EDA complexes of TNM with MPE and MPE-*d*₂ was performed in CH₂Cl₂ and acetonitrile as described above. The crude product obtained from the photolysis of 2'-(4-methoxyphenoxy)ethanol consisted of a 3:1 mixture of 2'-(4-methoxy-2-nitrophenoxy)ethanol and 2'-(4-methoxy-3-nitrophenoxy)ethanol (Table XIII). When the reaction was carried out in CH₂Cl₂ the isomer ratio changed to 3:2 in acetonitrile. The products were identified by comparison with that obtained from the nitration of 2'-(4-methoxyphenoxy)ethanol with fuming nitric acid. Thermal nitration yielded the 2-nitro and 3-nitro isomers in the ratio of 1.2:1, respectively. The pure 2-nitro and 3-nitro compounds were separated by column chromatography of the crude mixture on a silica gel column with a mixture of ether-petroleum ether as eluent (1:1 by volume). 2'-(4-Methoxy-2-nitrophenoxy)ethanol: yellow crystalline solid; mp 57–59 °C; IR (KBr) 3277 (s, OH), 3078 (s), 2937 (s), 2879 (w), 2836 (w), 1535 (s, NO₂), 1500 (s), 1453 (m), 1359 (s, NO₂), 1289 (s), 1223 (s), 1162 (m), 1083 (m), 1045 (s), 930 (m), 897 (m), 801 (s), 750 (m) cm⁻¹; ¹H NMR (CDCl₃) 7.37 (m, 1 H, H-3), 7.07 (m, 2 H, H-5, H-5,6), 4.18 (m, 2 H, OCH₂CH₂OH), 3.92 (m, 2 H, OCH₂CH₂OH), 3.80 (s, 3 H, OCH₃), 1.50 (br, 1 H, OH) ppm; ¹³C NMR (CDCl₃) 153.4 (OCH₃), 146.5 (OCH₂), 140.0 (C-2), 121.1 (C-6), 117.3 (C-5), 110.0 (C-3), 72.31 (OCH₂), 61.0 (CH₂OH), 56.0 (OCH₃) ppm; MS (70 eV) 213 (15, M⁺), 169 (100), 124 (13), 123 (10), 111 (20), 107 (15), 95 (10), 79 (27), 63 (13), 53 (15). 2'-(4-Methoxy-3-nitrophenoxy)ethanol: yellow crystalline solid; mp 76–78 °C; IR (KBr) 3304 (s, OH), 3195 (s, OH), 3082 (s), 3023 (m), 2941 (s), 1535 (s, NO₂), 1491 (m), 1451 (m), 1348 (s, NO₂), 1296 (s), 1275 (s), 1226 (s), 1176 (s), 1059 (s), 1019 (s), 961 (s), 900 (s), 869 (s), 806 (s), and 745 (s) cm⁻¹; ¹H NMR (CDCl₃) 7.40 (d, 1 H, H-2, *J* = 2.44 Hz), 7.16 (dd, 1 H, H-6, *J* = 2.49, 9.3 Hz), 7.01 (d, 1 H, H-5, *J* = 9.3 Hz), 4.02 (m, 4 H, CH₂CH₂OH), 3.91 (s, 3 H, OCH₃), 2.41 (br, s, 1 H, OH) ppm; ¹³C NMR (CDCl₃) 151.7 (C-4), 147.5 (C-1), 139.2 (C-3), 121.3 (C-5), 114.9 (C-6), 110.9 (C-2), 70.2 (OCH₂), 61.0 (CH₂OH), 56.9 (OCH₃) ppm; MS (70 eV) 213 (65, M⁺), 169 (91), 139 (22), 123 (10), 122 (65), 111 (21), 109 (59), 108 (40), 107 (15), 96 (10), 95 (15), 94 (16), 93 (59), 81 (15), 80 (15), 79 (38), 78 (11), 77 (13), 76 (27), 67 (13), 66 (19), 65 (62), 64 (15), 63 (31), 62 (15), 55 (14), 53 (46), 45 (100). Photolysis of EDA complex from 2'-(4-methoxyphenoxy)ethanol-1',1'-*d*₂ and TNM also yielded the corresponding 2-nitro and 3-nitro compounds in both CH₂Cl₂ and CH₃CN. The isomer ratio was identical with that obtained for the undeuterated compound. Analysis of the crude product by ¹H and ¹³C NMR indicated that there was no scrambling of the deuterium label between the 1'- and 2'-positions of the side chain during nitration. When the reaction was taken to partial completion and the unreacted starting material analyzed by ¹H and ¹³C NMR, no deuterium scrambling was found. Thermal nitration with nitric acid in acetic acid also yielded the 2-nitro and the 3-nitro compounds in the ratio of 55:45, respectively. In the electrophilic nitration, no deuterium scrambling was observed. 2'-(4-Methoxy-2-nitrophenoxy)ethanol-1',1'-*d*₂: ¹H NMR (CDCl₃) 7.39 (m, 1 H, H-3), 7.08 (m, 2 H, H-5,6), 4.16 (s, 2 H, OCH₂), 3.81 (s, 3 H, OCH₃), 2.57 (br, 1 H, OH) ppm; ¹³C NMR (CDCl₃) 153.4 (OCH₃), 146.4 (OCH₂), 139.8 (C-2), 121.2 (C-6), 117.2 (C-5), 109.8 (C-3), 72.1 (OCH₂), 60.3 (quintet, CD₂OH, *J*_{C-D} = 22 Hz), 55.9 (OCH₃) ppm; MS (70 eV) 215

(17, M⁺), 169 (100), 111 (18), 107 (12), 79 (18), 63 (12), 53 (13), 51 (14). 2'-(4-Methoxy-3-nitrophenoxy)ethanol-1',1'-d₂: ¹H NMR (CDCl₃) 7.39 (m, 1, 2-H), 7.08 (m, 2 H, H-5,6), 4.05 (s, 2 H, OCH₂), 3.90 (s, 3 H, OCH₃), 2.57 (br s, 1 H, OH), ppm; ¹³C NMR (CDCl₃) 151.8 (C-4), 147.7 (C-1), 139.3 (C-3), 121.4 (C-5), 115.1 (C-6), 110.9 (C-2), 70.06 (OCH₂), 60.3 (quintet, CD₂OH, J_{C-D} = 22 Hz), 57.0 (OCH₃) ppm; MS (70 eV) 215 (75), 169 (100), 139 (18), 123 (13), 122 (52), 111 (17), 109 (52), 108 (27), 107 (13), 95 (13), 94 (17), 93 (50), 81 (15), 80 (12), 79 (32), 77 (10), 76 (25), 67 (12), 66 (23), 65 (52), 64 (13), 63 (26), 62 (13), 53 (38), 52 (17), 51 (26), 47 (74).

3,4-Dimethoxyphenylacetonitrile. A solution containing 3,4-dimethoxyphenylacetonitrile (0.054 g, 0.3 mmol) and TNM (150 μL, 1.215 mmol) in CH₂Cl₂ (3 mL) was irradiated. The reaction was followed spectrophotometrically by the disappearance of the CT band. After 6 h of irradiation, the CT band had disappeared and during this period the solution had changed color from red-orange to yellow. The solvent and excess TNM was pumped off, and the resulting reddish-yellow oil was dissolved in CDCl₃ and CH₃NO₂ (10 μL) was added. The ¹H NMR spectrum of the crude product indicated the formation of only one aromatic product and HC(NO₂)₃ (7.94 ppm). The yield of the product was 94%. The solvent was pumped off, and the product was crystallized from a mixture of ether and hexane in the freezer. GC analysis of the crystallized product indicated only one peak, and it had the same retention time when coinjected with an authentic sample of 4,5-dimethoxy-2-nitrophenylacetonitrile. Also the ¹H NMR spectra of the two samples were identical. The authentic sample was obtained by thermal nitration of 3,4-dimethoxyphenylacetonitrile with fuming HNO₃ in ACOH in 80% yield.⁹² The crystallized product had mp 110–112 °C (lit.⁹³ mp 110–112 °C): IR (KBr) 2984 (m), 2949 (s), 2859 (m), 2258 (m, C≡N), 1579 (s, C=C), 1523 (s, NO₂), 1509 (s), 1406 (m), 1362 (m), 1331 (s, NO₂), 1275 (s), 1225 (s), 1059 (s), 984 (m), 867 (m), 797 (m), 755 (m) cm⁻¹; ¹H NMR (CDCl₃) δ 7.77 (s, 1 H, H-3), 7.09 (s, 1 H, H-6), 4.23 (s, 2 H, CH₂), 4.03 (s, 3 H, 5-OCH₃), 3.98 (s, 3 H, 4-OCH₃) ppm; ¹³C NMR (CDCl₃) 153.8 (C-5), 148.8 (C-4), 139.9 (C-2), 120.2 (C-1), 116.8 (CN), 112.1 (C-6), 108.7 (C-3), 56.7 and 56.5 (4- and 5-OCH₃), 23.0 (CH₂) ppm; MS (70 eV) 223 (5, M + 1), 222 (46, M), 206 (12), 205 (100), 177 (18), 160 (23), 151 (16), 149 (14), 136 (23), 133 (16), 132 (44), 131 (28), 130 (17), 118 (17), 103 (16), 90 (24), 89 (15), 77 (33), 76 (28), 75 (17), 64 (28), 63 (65), 62 (25), 53 (25), 51 (23), and 50 (33).

1,3,5-Trimethoxybenzene (TMB). A solution containing 1,3,5-TMB (0.025 g, 0.15 mmol) and TNM (40 μL, 0.33 mmol) in CH₂Cl₂ (3 mL) showed the charge-transfer band in the electronic spectrum as a shoulder tailing up to 600 nm. The solution was irradiated with a focussed beam from a 500-W Hg lamp fitted with a 425-nm Corning cutoff filter and an aqueous IR cutoff filter. Upon irradiation, the solution changed color from orange-red to pale green and then gradually to dark greenish-blue. The color change was followed by UV-vis spectroscopy, which indicated the growth of an intense band at 615 nm (λ_{max}) which overlapped with the CT band. After 2 h, the irradiation was stopped and the solvent and excess TNM were removed in vacuo. Analysis of the dark greenish-blue semisolid residue indicated the presence of mainly the starting material.

2,6-Dimethoxytoluene (DMT). A solution containing 2,6-DMT (0.045 g, 0.29 mmol) and TNM (100 μL, 0.8 mmol) in CH₂Cl₂ (3 mL) was irradiated with a focussed beam from a 1000-W Hg lamp as described above. The color of the solution gradually changed from amber to bluish green. After 1.5 h, the solution was very dark bluish-green. Further irradiation up to 4 h yielded a dark-red solution. The solution was worked up as described above. The crude material by ¹H NMR and GC

analysis consisted of the starting material as the major component and three other products. One of the products showed a mass spectrum with *m/z* 197 (mass ion of the nitro compound).

The charge-transfer nitrations of 1,2-dimethoxybenzene and 3,5-dimethoxyphenylacetonitrile were described previously.¹⁶

Quantum Yield for the Charge-Transfer Nitration. Owing to the strong similarities of the various aromatic ethers in charge-transfer nitration, 1,4-dimethoxybenzene was chosen for a detailed study in various solvents. The quantum yields were measured with a 500-W high-pressure mercury lamp focussed through an aqueous IR heat filter, followed by a 520-nm interference filter (10-nm band pass) used as a monochromator. Calibration of the lamp was performed with a Reinecke salt actinometer, as described by Wegner and Adamson.⁴⁴ In a typical experiment, a 2-mL solution of 1,4-DMB and excess TNM with tetradecane as the internal standard was placed in a 1-cm quartz precision cell, which was irradiated for a given period of time. The absorbance of the solutions at 520-nm was ≈ 2.0 to ensure the complete absorption of the light. Conversions were kept to 10–15%. After photolysis, the photolysate was quantitatively analyzed by GC for 2,5-dimethoxynitrobenzene and 1,4-DMB. The molar response factors of 2,5-dimethoxynitrobenzene and 1,4-DMB with respect to tetradecane were obtained by separate GC analyses and found to be reproducible to within ±10%. The quantum yield of formation of 2,5-dimethoxynitrobenzene and disappearance of 1,4-DMB were obtained from individual experiments (Table IX).

Kinetic Isotope Effect for Charge-Transfer Nitration of *p*-Dimethoxybenzene. A solution containing a mixture of 1,4-DMB (13.8 mg, 0.1 mmol) and 1,4-DMB-*d*₄ (14.2 mg, 0.1 mmol) was prepared in CH₂Cl₂ (3 mL). The relative amounts of 1,4-DMB and 1,4-DMB-*d*₄ in the mixture were determined by GC-MS analysis by using the relative abundance of the molecular ion peaks (*m/z* 138 and 142, respectively), i.e., φ(DMB)₀ = [abundance of *m/z* = 138]/[abundance of *m/z* = 142] = 54/42 = 1.04. An aliquot of TNM (100 μL, 0.8 mmol) was added to the mixture and photolysis was carried out with a focussed beam from a 500-W Hg lamp equipped with an infrared water filter and a 425-nm cutoff filter. Photolysis was carried out for 1 h, and the decrease in the intensity of the CT band was followed spectrophotometrically. The absorbance of the CT band at 550 nm before and after photolysis was 0.304 and 0.128, respectively, at 70% conversion. The solvent and excess TNM were removed in vacuo. The mixture was dissolved in CDCl₃ and subjected to ¹H NMR analysis. It indicated a mixture consisting of 75% product and 25% starting material. GC and ²H NMR analysis were consistent with this result and indicated 75% and 76% conversion, respectively. The relative amounts of the unreacted 1,4-DMB and 1,4-DMB-*d*₄ and that of the products 2,5-dimethoxynitrobenzene and 2,5-dimethoxynitrobenzene-*d*₃ were determined by GC-MS analysis by using peaks *m/z* 138 and 142 for starting materials, i.e., φ(DMB) = [abundance of *m/z* = 138 after photolysis]/[abundance of *m/z* = 142 after photolysis] = 49/52 = 0.94, and for the products, i.e., φ(DMB-NO₂) = [abundance of *m/z* = 183]/[abundance of *m/z* = 186] = 92/91 = 1.01.

A similar procedure was followed to measure the quantum yields and low conversion. Thus the 1000-W Hg lamp with the 425-nm cutoff filter was used to irradiate the solution for 12 min. ¹H NMR analysis of the reaction mixture indicated 82% unreacted starting material and 18% product: for φ(DMB)₀ = 0.95, it was found that φ(DMB) = 0.95 and φ(DMB-NO₂) = 1.09.

Acknowledgment. We thank S. J. Atherton and M. A. J. Rodgers of the Center for Fast Kinetics Research (under support from NIH Grant RR00886 and the University of Texas, Austin) and the National Science Foundation and the Robert A. Welch Foundation for financial support.

(92) Stamos, I. K. *Synthesis* 1980, 663-4.

(93) Walker, G. N. *J. Am. Chem. Soc.* 1955, 77, 3844 and also ref 1.